HHS Public Access

Author manuscript

Brain Res. Author manuscript; available in PMC 2019 May 15.

Published in final edited form as:

Brain Res. 2014 October 02; 1583: 89–108. doi:10.1016/j.brainres.2014.07.022.

Forelimb amputation–induced reorganization in the ventral posterior lateral nucleus (VPL) provides a substrate for large-scale cortical reorganization in rat forepaw barrel subfield (FBS)

Cheng X. Li, **Tyson D. Chappell**, **John T. Ramshur**, and **Robert S. Waters***

Department of Anatomy and Neurobiology, University of Tennessee Health Science Center, College of Medicine, 855 Monroe Avenue Memphis, TN 38163, USA

Abstract

In this study, we examined the role of the ventral posterior lateral nucleus (VPL) as a possible substrate for large-scale cortical reorganization in the forepaw barrel subfield (FBS) of primary somatosensory cortex (SI) that follows forelimb amputation. Previously, we reported that, 6 weeks after forelimb amputation in young adult rats, new input from the shoulder becomes expressed throughout the FBS that quite likely has a subcortical origin. Subsequent examination of the cuneate nucleus (CN) 1 to 30 weeks following forelimb amputation showed that CN played an insignificant role in cortical reorganization and led to the present investigation of VPL. As a first step, we used electrophysiological recordings in forelimb intact adult rats (n=8) to map the body representation in VPL with particular emphasis on the forepaw and shoulder representations and showed that VPL was somatotopically organized. We next used stimulation and recording techniques in forelimb intact rats (n=5) and examined the pattern of projection (a) from the forelimb and shoulder to SI, (b) from the forepaw and shoulder to VPL, and (c) from sites in the forepaw and shoulder representation in VPL to forelimb and shoulder sites in SI. The results showed that the projections were narrowly focused and homotopic. Electrophysiological recordings were then used to map the former forepaw representation in forelimb amputated young adult rats (n=5) at 7 to 24 weeks after amputation. At each time period, new input from the shoulder was observed in the deafferented forepaw region in VPL. To determine whether the new shoulder input in the deafferented forepaw VPL projected to a new shoulder site in the deafferented FBS, we examined the thalamocortical pathway in 2 forelimb-amputated rats. Stimulation of a new shoulder site in deafferented FBS antidromically-activated a cell in the former forepaw territory in VPL; however, similar stimulation from a site in the original shoulder representation, outside the deafferented region, in SI did not activate cells in the former forepaw VPL. These results suggest that the new shoulder input in deafferented FBS is relayed from cells in the former forepaw region in VPL. In the last step, we used anatomical tracing and stimulation and recording techniques in forelimb intact rats (n=9) to examine the cuneothalamic pathway from shoulder and forepaw receptive field zones in CN to determine whether projections from the

* Corresponding author at: Department of Anatomy and Neurobiology, University of Tennessee Health Science Center, College of Medicine, 855 Monroe Avenue, Memphis, TN 38163, USA rwaters@uthsc.edu FAX: (901) 448-7193.

shoulder zone might provide a possible source of shoulder input to forepaw VPL. Injection of biotinylated dextran amine (BDA) into physiologically identified shoulder responsive sites in CN densely labeled axon terminals in the shoulder representation in VPL, but also gave off small collateral branches into forepaw VPL. In addition, microstimulation delivered to forepaw VPL antidromically-activated cells in shoulder receptive field sites in CN. These results suggest that forepaw VPL also receives input from shoulder receptive sites in CN that are latent or subthreshold in forelimb intact rats. However, we speculate that following amputation these latent shoulder inputs become expressed, possibly as a down-regulation of GABA inhibition from the reticular nucleus (RTN). These results, taken together, suggest that VPL provides a substrate for large-scale cortical reorganization that follows forelimb amputation.

Keywords

Somatosensory cortex; SI; forepaw barrel subfield; FBS; ventral posterior lateral nucleus; VPL; reticular nucleus; RTN; cuneate nucleus; dorsal column nuclei; forepaw representation; forelimb amputation; forelimb deafferentation; rat

1. Introduction

We previously described the morphological and physiological organization of the forepaw and wrist representations (Waters et al., 1995) and forelimb and shoulder representations (Pearson et al., 1999) in adult rat primary somatosensory cortex (SI). SI contains clusters of cells in layer IV, called barrels, that are associated with the representation of the glabrous digits, digit pads, and palmar pads and together form the forepaw barrel subfield (FBS). The representations of the wrist, arm, and shoulder (hereafter call the original shoulder) lie posterior to the FBS. We reported that 4-5 weeks after forelimb amputation new long-latency responses from the shoulder were recorded in the deafferented forepaw region in SI (Pearson et al., 2003). These new shoulder inputs are not derived from horizontal projections from the original shoulder representation in SI or from the second somatosensory cortex (SII) (Pearson et al., 2001). The results suggest that large-scale cortical reorganization quite likely involves a subcortical substrate as suggested by others (Garraghty and Kaas, 1991; Rasmusson, 1996a; Stojic et al., 1998).

The cuneate nucleus (CN) and ventral posterior lateral nucleus (VPL) are somatotopically organized and play important roles in processing and relaying ascending information to SI and are therefore very likely involved in large-scale cortical reorganization that follows forelimb amputation. The physiological representation of the forelimb in rat CN was described by Nord (Nord, 1967) and subsequently confirmed, in large part, by others (Li et al., 2012; Maslany et al., 1990). CN contains a centralized cluster of cells associated with the representation of the forepaw and an adjacent non-cluster region representing the wrist, arm, and shoulder (Crockett et al., 1993; Li et al., 2012; Maslany et al., 1990). Following forelimb amputation in young adult rats, little or no new shoulder input was found within the central forepaw region up to 30 weeks post amputation, suggesting that CN provides an unlikely substrate for large-scale reorganization in the FBS (Li et al., 2013). This finding is consistent with a number of studies that reported an insignificant role for CN in providing a

substrate for cortical reorganization that follows forelimb amputation (Bowlus et al., 2003; Lane et al., 2008).

The morphological (Belford and Killackey, 1978) and physiological (Angel and Clarke, 1973; Angel and Clarke, 1975; Emmers, 1965; Francis et al., 2008) organizations of the cutaneous forelimb and shoulder representations have been similarly described in VPL in rats. More recently, a detailed somatotopic map of the cutaneous forelimb representation in rat VPL has been elucidated (Francis et al., 2008). While reorganization has been reported in ventral posterior medial nucleus (VPM) following manipulation of the whiskers, few studies have examined VPL reorganization following forelimb amputation, and these have been conducted in rats undergoing amputations as neonates (Stojic et al., 1998). In contrast, reorganization in VPL has been reported following digit amputation in raccoon (Rasmusson, 1996a; Rasmusson, 1996b) and sectioning of peripheral afferents in monkey (Garraghty and Kaas, 1991).

The present experiments were conducted to (a) examine the organization of VPL in forelimb intact rats, (b) examine the reorganization in VPL following forelimb amputation in young adult rats, (c) test whether shoulder-responsive regions in deafferented forepaw VPL project to shoulder responsive sites in the deafferented FBS, and (d) examine the origin of the new shoulder inputs in deafferented VPL.

2. Results

In total, 29 Sprague-Dawley rats were used in this study. Of that number, VPL was mapped in 8 forelimb intact adult controls. In 5 rats, the forelimb was deafferented between 7–8 weeks of age and VPL was mapped between 7–24 weeks after amputation. Projections from deafferented VPL to SI were examined in 2 rats. Projections from the periphery to VPL and to SI were examined in 5 forelimb intact rats, and the cuneothalamic pathway was studied with anatomical tracer (n=5) and electroanatomy (n=4).

2.1 Organization of forelimb and shoulder representations in VPL

The organization of VPL in forelimb intact control rats was examined to provide a generalized map of the forelimb and shoulder to guide us in comparing controls with forelimb amputees. Full maps were generated in 3 forelimb intact control rats and partial maps that focused on exploration of the shoulder and/or forepaw representation were examined in an additional 5 animals. An example of the results from 3 mapping experiments along with an interpretative summary of the forelimb/shoulder representation in VPL is presented in Fig. 1. A reconstruction of a series of electrode penetrations through VPL and recorded receptive fields is illustrated in Fig. 1A. The inset depicts a photomicrograph of a cytochrome oxidase (CO)–stained coronal section through the region studied along with 2 electrode tracks (lines) showing the locations where lesions (open circles) were made to aid in map reconstruction. The line drawing shows the locations of 8 electrode penetrations that passed through the VPL and/or VPM. In penetration nos. P1–P6, the electrode passed through VPM where it encountered receptive fields of vibrissae and/or lower lip. At more ventral locations, the electrode entered VPL where the representations of the forepaw, digit and palmar pads, wrist, and dorsal hand were found. Within VPL, digit 1 (D) is represented

ventromedially and is followed dorsolaterally by a serial progression of the representation of D2 through D5. The thenar pad (TH) representation lies below D1 and the hypothenar pad (HT) lies below the D5 representation. The digit pad (P1, P2, P3) representations lie below the digit representations in between the TH and HT pad representations. Electrode penetration no. 6 entered VPL dorsally and immediately encountered a site that responded to vibrissae and shoulder stimulation. Within the next 400 microns, receptive fields were only found on the shoulder. The electrode then entered sites responsive to input from the arm (A), chest (Ch), and abdomen (Ab) before entering into the forelimb representation where receptive fields were immediately found on dorsal hairy skin of D5 (D5d) and dorsal hand (Hd). With the further advancement of the electrode, receptive fields were recorded on dorsal D5 (D5d) and hypothenar pad (HT). Upon entry of electrode penetrations nos. 7 and 8 into VPL, receptive fields were recorded on the back (B) and side (S); the electrode then passed into the hindlimb (HL) representation. From this map, VPL appears to be somatotopically organized into forepaw, arm, shoulder, trunk, and hindlimb zones. The wrist representation very likely overlaps with the forepaw and arm zones, and chest and abdomen representations are quite likely part of the trunk zone and/or comprise separate smaller zones. Within the forepaw zone, the forepaw digits are represented ventrally and extend dorsally immediately below the border of the neighboring VPM, and the pad representations lie immediately below these digit representations.

A map from a second rat is presented in Fig. 1B along with a photomicrograph showing the location of recovered lesion sites along 2 of the electrode penetrations. The same common plan of somatotopic organization was also seen in this animal. The forepaw representation lies most ventral and is separated from the shoulder representation by the representation of arm. In this example, no electrode penetration passed through the D1 representation, but D1 was found in this location in several of the partially mapped rats (data not shown). From the VPL map in this second rat, it is clear that the forepaw is represented most ventrally and is separated from the shoulder representation by the arm and trunk representations.

The reconstructed zones of the body representation (forepaw, arm, shoulder, trunk, and hindlimb) from the above examples along with the reconstruction from a third rat are shown in Fig. 1C. These zones were then superimposed on one another and a best-fit line was drawn to produce a composite map that is shown at right, along with our interpretation of the zonal organization (Fig. 1C). These zones were then fitted to a standardized map of VPL that was derived from producing a best fit (inset in Fig. 1D) from reconstructions of combined VPM, VPL, and RTN nuclei from the 3 rats. The important feature to note is the general somatotopy of the forelimb-shoulder representation where the forepaw representation lies most ventral and is separated from the shoulder representation by the arm representation at a distance of approximately 400– 600 microns. In none of these cases did we ever encounter an overlap between the forepaw and shoulder representations in forelimb intact rats.

2.2. Forelimb and shoulder projections to SI cortex

Stimulation and recording techniques were used to examine the pattern of projection between periphery and SI in 2 intact control rats. We used similar techniques to examine the pattern of projection between forepaw and shoulder representations in VPL and forelimb and

shoulder representations in SI. These studies were carried out in forelimb intact rats to determine if the projection pattern to SI from periphery and VPL was focal or wide spread, which would be useful later for interpreting reorganization in forelimb amputees.

2.2.1. – Forelimb and shoulder project to their respective homotopic sites in SI cortex—The projection pattern from periphery to SI was studied in 2 intact control rats. The forepaw, wrist, arm, and shoulder representations were initially mapped in SI using mechanical stimulation, and their locations were plotted on a digital map of the brain surface. A stimulating probe consisting of a twisted pair of silver wires was then placed at a selected site on the forelimb or shoulder and used to examine input from the periphery to each of the mapped sites in SI. An example of the stimulating paradigm and physiological recordings is shown in Fig. 2 for 1 rat. In this experiment, the location of the representations of the TH pad, digit 3 ventral proximal (D3vp), D3 ventral tip (D3vt), D5vt, wrist, forearm, upper arm, and shoulder were initially mapped in SI cortex using mechanical stimulation. A stimulating probe was then placed on the skin surface on the glabrous tip of D3 and used to deliver single pulses (1-ms duration), and evoked responses were examined at each previously recorded site in SI. An example of a short-latency response (7.5 ms) was recorded at the D3vt location in SI. Stimulation current was then increased from 1.5 × threshold to 3 × threshold and used to examine evoked response input to each of the previously mapped cortical sites. Stimulation of D3vt was also effective in evoking a cortical response at the representation of the proximal part of digit 3 (D3vp). Peripheral stimulation of D3 evoked cortical responses at only these 2 recording sites in SI, and this is indicated by the solid lines labeled 2 and 3 in Fig. 2. Dashed lines indicate nonresponsive stimulating and recording locations. On the outer border of the figure, averaged oscilloscope traces are presented for each stimulating and recording site. Those traces where evoked responses were recorded are demarcated by an oval over the relevant portion of the trace, and an inset is shown that displays a buffer of 10 consecutive stimulations. The stimulating probe was then moved to a site on the shoulder that was previously effective in evoking a response in the shoulder cortex; this stimulation site was then used to examine evoked response at each cortical location. Stimulation of the shoulder was effective in evoking responses only from shoulder cortex and from an adjacent region in which both shoulder and upper arm receptive fields were recorded. Solid lines designated as “A and B” show these projections. Evoked response records are shown at the perimeter in “A” and “B”. These results support the notion that the projections from forepaw and shoulder periphery to SI are homotopic and restricted to narrow regions within their respective forepaw and shoulder representation in SI.

2.2.2. – Shoulder and forepaw project only to their respective homotopic sites in VPL—We examined the projection from forepaw and shoulder to forepaw and shoulder receptive field locations in VPL in 5 forelimb intact rats using the stimulating and recording techniques previously described. An example of these results is shown in Fig. 3. In this example, the electrode in the thalamus recorded receptive fields on D1 and TH pad. Stimulation of the skin surface on D1 or TH evoked a short-latency response (5.75 ms) in VPL at 1.5 × threshold stimulation current. When the electrode was moved to sites in the shoulder representation, peripheral stimulation of D1 or TH failed to evoke a response even at amplitudes greater than 3 × threshold. When the stimulating electrode was placed on the

shoulder, a short-latency response was evoked at the shoulder region in VPL; however, stimulation failed to evoke a response at the forepaw region in VPL. These results suggest that the projection from periphery to VPL is also focal and homotopic.

2.2.3. – Shoulder and forepaw sites in VPL project to homotopic sites in SI—

The recording electrode in VPL was then used for stimulation (Fig. 3 top). Locations of the D1/TH and shoulder representations in SI were then identified and used to record responses following stimulation of shoulder and D1/TH sites in VPL. Stimulation in the shoulder representation in VPL evoked a short-latency response in the shoulder representation in SI, but did not evoke a response in the digit representation in SI. Similarly, stimulation of D1/TH site in VPL evoked a vigorous response in the digit representation in SI, but failed to evoke a response in shoulder cortex. The electrode in D1/TH cortex was then used to deliver single pulses to the recording site in VPL to search for antidromically-activated responses. An example of an antidromically-activated response is shown in the figure inset labeled “A”; the averaged spike for 10 stimulations is shown along with a buffer of 10 spikes. Similar stimulation in shoulder cortex failed to evoke antidromic responses at the D1/TH location in VPL.

These results, summarized in Table 1, suggest that projections from periphery to VPL and SI and from VPL to SI are topographically organized, narrowly focused, and unlikely to sprout to the extent necessary to form a substrate for large-scale cortical reorganization after forelimb amputation.

2.3 After forelimb amputation, neurons in the former forepaw zone in VPL respond to new inputs from the shoulder

VPL organization was examined in 5 rats at 7–24 weeks after forelimb amputation, and these results are illustrated in Fig. 4. The map illustrated in Fig. 4A was recorded 7 weeks after amputation and shows a series of 7 electrode penetrations through VPL. Each small black circle along the penetration corresponds to a recording site; however, only those sites where receptive fields were recorded on the shoulder are illustrated. Within VPL, the 2 most ventral recording sites in penetration no. 4 encountered receptive fields on shoulder, and these sites are located within the presumptive former forepaw representation. Penetrations nos. 5–7 in the dorsal part of VPL encountered several sites that received input from the shoulder, and these sites were located, in large part, in the original shoulder representation. In penetration no. 7, receptive fields were also recorded on the trunk and hindlimb, but these are not included to emphasize the relationship between the forepaw and shoulder responsive sites. The map illustrated in Fig. 4B was generated from a rat at 18 weeks after amputation. New shoulder input was recorded in the presumptive forelimb region in the thalamus. Note in this example, the shoulder representation was also found in a bordering site in the adjacent VPM. The map illustrated in Fig. 4C was generated in a rat that was mapped 24 weeks after amputation; note that the size of the shoulder representation occupied a large part of the presumed glabrous digit zone in VPL. No attempt was made to map the original shoulder representation in these 2 rats, although 1 electrode track (penetration No. 5 in Fig. 4C) recorded input from the shoulder. The photomicrographs in the upper right corners show locations where lesions were made along a penetration to aid in electrode reconstructions.

The maps from these reconstructions are redrawn in Fig. 4D, and another map from an 8-wk deafferented rat has been added. The locations of the shoulder representations have been merged onto the standardized drawing (from Fig. 1D), and these are illustrated in Fig. 4E. Note that these new shoulder representations are found in the ventromedial portion of VPL that is associated with the representation of forepaw in the intact rat as illustrated in Fig. 1D.

2.4. VPL provides a substrate for large-scale cortical reorganization in the FBS

VPL and SI connectivity were studied in forelimb amputees (n=2) to determine whether new shoulder sites in VPL and deafferented FBS share a common projection. An example from 1 rat is illustrated in Fig. 5. The original and new shoulder representations in SI were identified using mechanical and electrical stimulation. The new shoulder recording site is shown in CO-stained flattened section in Fig. 5A and corresponds to the location of barrels associated with the representation of D1/TH; recording site marked by a lesion (arrowhead) in Fig. 5A. Locations of the new shoulder representation in the FBS (arrowhead) and the original shoulder representation are shown in the line drawing in Fig. 5B. The right side of the figure, drawn with solid lines, is the reconstruction from the flattened section in Fig. 5A. The left side of the figure drawn with dashed lines, represents our best estimate of the shape of the barrel field and the approximate location of the original shoulder representation in SI based on the point of entry of the recording electrode as it passed through the cortical surface. The brain was blocked at the interface between the solid and dashed lines, and the posterior part (dashed lines) was sectioned in a coronal plane.

In this rat, an electrode was inserted into VPL and lowered to the presumptive former location of D1 and TH where receptive fields on the shoulder were identified. This recording site is shown in the coronal section in Fig. 5C and the line drawing in Fig. 5D. A stimulating probe was then placed on the shoulder skin and used to deliver single-pulse stimulation (1.0-ms duration; 1 Hz interval) and a short-latency response was recorded at the original shoulder site (Fig. 5E), and a delayed response was recorded in the FBS shown in Fig. 5F, similar to our previous finding (Pearson et al., 1999). To determine whether shoulder site in the presumptive forepaw region VPL projected to the new shoulder site in the FBS, we stimulated SI and recorded an antidromically-activated response at the new shoulder site in VPL as shown in Fig. 5G. However, when the original shoulder in SI was stimulated, we were unable to antidromically activate neurons in the presumptive forepaw site in VPL and this result is shown in Fig. 5H.

These results suggest that, following deafferentation, VPL reorganizes and that neurons in the forepaw region that were previously responsive to input from the forepaw become responsive to new input from the shoulder. These shoulder responsive sites in the presumptive former forepaw territory in VPL quite likely project to SI over the same pathway that previously carried input from the forepaw. Following deafferentation, this pathway now conveys new input from the shoulder and very likely provides a substrate for new shoulder input to deafferented cortex following forelimb amputation.

2.5. Cuneothalamic projections from shoulder responsive sites in CN may provide a source of latent shoulder input to forepaw VPL that becomes expressed following deafferentation

Following forelimb amputation, neurons in the former forepaw representation in VPL become responsive to new input from the shoulder. We previously provided evidence that the former forepaw area in CN does not become responsive to new shoulder input following amputation and therefore is an unlikely source of new shoulder input to the deafferented VPL (Li et al., 2013). Therefore, what is the source of the new shoulder input to VPL? In the present study, we addressed this question by examining the projection from the shoulder representation in CN in forelimb intact rats using anatomical tracing and electroanatomy techniques. Our findings suggest that cuneothalamic pathway may provide a latent source of shoulder input to forepaw VPL that becomes expressed following forelimb amputation.

2.5.1. –Anatomical tracing—The anterograde tracer biodextran amine (BDA) was used to examine the projection from CN to VPL in 5 rats. In 2 rats, injections were made into physiologically identified sites in the shoulder representation; and in 3 rats, injections were made into the forelimb representation. An example of the results from 1 rat where the injection was localized to the shoulder representation within the tail zone of CN is illustrated in Fig. 6. In this rat, 4 electrode penetrations were required to find the shoulder representation, which appeared at a depth of 375 μm below the brainstem surface. The recording electrode was then replaced by a micropipette containing a 2% solution of BDA that was iontophoresed for a total of 10 minutes (1-μA injection current, 7-sec duty cycle). A photomicrograph of the injection site is shown in Fig. 6A; the dashed oval shows the inner dense core of labeling which was located in the tail region of CN where the shoulder (SH) representation was found. The inset shows the surface entry location for the injection (arrowhead) in relationship to the obex (dashed line). A summary map showing the general representation of the forelimb in rat VPL is presented in the line drawing in Fig. 6B (from Fig. 1D). It is important to note that the forepaw (FP) representation is located ventromedial and is separated from the dorsolaterally located shoulder (SH) representation by the wrist (W) and arm (Arm) representations; the dorsal edge of the FP is separated from SH by approximately 400 μm. In this rat, extensive terminal labeling was found in the region of shoulder representation in VPL (enclosed oval region), and this is shown in the photomicrograph in Fig. 6C. In the photomicrograph from the adjacent section, axons can be seen throughout the forepaw (FP) region (boxed region) as shown in Fig. 6D, and at higher resolution in Figs. 6E, 6F. The inset in Fig. 6F shows an axonal branch in FP. Scattered axons can also be seen throughout FP.

2.5.2. –Electroanatomy tracing—Extracellular recording and microstimulation were used to reexamine the connection between CN and VPL in 4 forelimb-intact rats. In 2 rats, the connection was studied between physiological sites in the shoulder representation in CN and the forepaw representation in VPL; in 2 other rats, the connection was examined between physiological sites in the forelimb representation in CN and the shoulder representation in VPL. The connection between the shoulder representation in CN and the forepaw representation in VPL in 1 rat is shown in Fig. 7. In this example, a microelectrode was inserted into VPL, and the electrode was lowered into the forepaw representation where

a receptive field was recorded on D3; the electrode was then fixed in place. A second microelectrode was inserted into the tail region in CN and used to record receptive fields of neurons along the penetration. At a depth of 400 μm, a clear receptive field was identified on the shoulder in CN. The recording site in CN is shown in the sagittal section (arrow) in Fig. 7A. The location of surface point of entry for the electrode (black circle with arrowhead) is shown in the left inset in relationship to the obex (dashed line). The location of the thalamic stimulating electrode (open circle) that also marks the site of a lesion is shown in the right inset: the electrode path (pale line) can also be seen extending through VPL. The thalamic electrode was then used to deliver microstimulation (1-ms duration, at 1 Hz), and an antidromically-activated response (stimulation amplitude, 16 μA) was recorded in CN; a single evoked response (arrowhead) is shown in Fig. 7C (left), averaged evoked response following 10 stimulus pulses is shown in 7C (center), and a 10-trace buffer is shown in Fig. 7C (right). This cell was antidromically-activated and had an invariant latency of 3.16 ms following rapid stimulation; the inset in Fig. 7C shows a single evoked response (arrowhead). The extracellular electrode was then withdrawn and replaced with an intracellular electrode that was inserted into the approximate brainstem location as the extracellular electrode and lowered into CN. At a depth of 420 μm, a cell was impaled that had a receptive field on the shoulder. Microstimulation was delivered to the thalamic electrode and an antidromically-activated evoked responses was recorded; examples of responses are shown in Fig. 7D for a single trace (left), 10 averaged traces (center), 10-trace buffer (right). The cell was injected for 10 minutes and the location of the labeled cell in CN is shown in the line drawing in Fig. 7B, and the labeled cell is shown in the inset. This cell had an evoked response latency of 3.62 ms. Extracellular evoked response data are not shown for the CN-shoulder to VPL-forepaw connection in the second rat where an averaged evoke response latency of 3.47 ms was recorded.

3. Discussion

The present findings support the conclusion that VPL provides a substrate for large-scale cortical reorganization in rat SI (Pearson et al., 1999) that takes place after forelimb amputation. To reach that conclusion we (a) examined the organization of forelimb and shoulder representations in VPL in forelimb intact rats, (b) determined the pattern of peripheral input from the forelimb and shoulder to VPL and SI and the pattern of input from forepaw and shoulder regions in VPL to SI cortex, (c) examined the organization in VPL in forelimb amputated young adult rats 7–24 weeks after amputation, (d) tested those sites in deafferented forepaw VPL that responded to new input that relayed that same input to deafferented SI, and (e) presented data suggesting that CN provides a latent source of new shoulder input to VPL that becomes expressed following forelimb amputation.

Previously, we reported that 4–5 weeks after forelimb amputation, new input from the shoulder appeared in the deafferented FBS (Pearson et al., 2003) and by 6 weeks after amputation, the new shoulder input occupied most of the FBS (Pearson et al., 1999). Ablation of the original shoulder representation in SI and/or SII failed to eliminate the new shoulder input, suggesting that large-scale cortical reorganization in the FBS was most likely mediated at the subcortical level (Pearson et al., 2001).

To address the possibility that subcortical circuits underlie the observed reorganization in SI, we began by studying the organization (Li et al., 2012) and reorganization (Li et al., 2013) of CN with the prediction that CN would show a parallel pattern of reorganization similar to that observed in SI. Like SI, CN contains clusters that are associated with the representation of the forepaw digits and pads, but unlike SI, significant new input from the shoulder was not observed within this forepaw region up to 30 weeks after amputation. The absence of new shoulder input into the deafferented forepaw zone in CN was unexpected, since we predicted that the reorganized forepaw zone in CN would provide the source of new shoulder input to VPL over the well-established cuneothalamic pathway between the forepaw zone in CN and forepaw zone in VPL (Alloway and Aaron, 1996). We interpreted these findings as evidence that CN was an unlikely source of new shoulder input to the deafferented VPL.

In the present study, evidence was provided that the former forepaw region in VPL becomes responsive to new input from the shoulder after forelimb amputation, and relays this new shoulder input to deafferented FBS. Since cuneothalamic projections from deafferented forepaw zone in CN could be ruled out as the source of new shoulder input to VPL that follows forelimb amputation, we reexamined the cuneothalamic projection in forelimb intact rats. In so doing, we observed that forepaw and shoulder regions of CN projected primarily to homotopic sites in VPL, but they also gave off collateral branches to non-homotopic sites that were unexpressed in forelimb intact rats. We speculate that following amputation, these latent shoulder inputs become expressed in the deafferented forepaw region in VPL.

3.1 Organization of VPL in rat

The present findings revealed a clear somatotopic representation of the limb and trunk body surface in VPL. Specifically, we were interested in identifying the location of the forepaw and shoulder representation in forelimb intact rats. Mapping was restricted to the middle cutaneous portion of VPL as previously described (Francis et al., 2008), where receptive fields are narrow and a nearly complete body representation can be mapped in a single medial to lateral row of electrode penetrations through VPL. This latter fact is important for subsequent comparison of maps in forelimb amputees since it is difficult to reconstruct the cell cluster arrangement in the forepaw portion of VPL as a result of the numerous fibers that project through this region.

In rat VPL, the forepaw glabrous digits are represented ventrally; digit 1 (D1) is represented most ventromedial followed serially in a dorsolateral direction by the representation of D2–D5. The digit and palmar pads are represented directly beneath the digit representations with the thenar pad (TH) representation directly below D1 and the hypothenar pad (HT) representation below D5. The representation of digit pads P1–P3 lay between TH and HT pads. We speculate that a somatotopic organization exists within a single digit representation (D2–D5) where the proximal part of the digit representation lies closest to the pads and the distal part of the digit representation lies in close proximity to VPM; in this arrangement, the dorsal hairy digit skin lies immediately adjacent to VPM. A similar somatotopic organization for D2–D5 was previously reported in rat CN (Li et al., 2012) and FBS (Waters et al., 1995). The wrist and arm representations extend in a dorsolateral direction from D5

and together with the forepaw representation make up the forelimb zone. The shoulder representation lies immediately dorsolateral to the forelimb representation. In the forelimb intact rat, receptive fields for the shoulder were never encountered in the forepaw territory, nor were receptive fields for the forepaw ever observed in the shoulder territory in VPL.

The somatotopic organization of the ventrobasal (VB) thalamus, that includes VPM and VPL, has been previously reported (Davidson, 1965; Emmers, 1965; Jaw et al., 2008; Wall and Egger, 1971). Most recently, the organization of VPL in rat was described in detail (Francis et al., 2008). They reported that VPL was partitioned into 3 well-defined zones: a rostral zone (VPLr) that carried primarily proprioceptive and large receptive field cutaneous information, a middle zone (VPLm) that received small receptive field cutaneous input for the dorsal column, and a caudal zone (VPLc) that received large receptive field cutaneous input derived in large part from the spinothalamic tract. Our maps were made entirely within VPLm and are in good agreement with their summary map of the forelimb representation (see Figure 6 in Francis et al., 2008).

3.2 Reorganization of VPL in rat following forelimb amputation

Once locations of forepaw and shoulder representations were identified in the intact rat, the appearance of new shoulder input in the former forepaw zone in VPL provided evidence for reorganization in VPL following forelimb amputation.

3.2.1 – Reorganized maps in forelimb VPL—In the present study, the forelimb was amputated in young adult rats and VPL was mapped 7-to 24-weeks after amputation. In all cases, new shoulder input was recorded in the deafferented forepaw region in VPL that was not present prior to amputation. The location of the original shoulder representation in rat VPL is greater than 400 μm dorsolateral to the forepaw representation and is separated by representations of wrist and arm.

We are unaware of previous studies in rat where VPL organization was examined following forelimb amputation in young adult or adult rats. In contrast, investigators have examined VPL following neonatal forelimb amputation in rat (Stojic et al., 1998), digit amputations in raccoon (Rasmusson, 1996a; Rasmusson, 1996b), peripheral nerve section in non-human primate (Garraghty and Kaas, 1991), and whisker deafferentation in mice (Verley and Onnen, 1981). In these studies, the general finding is that the VPL map reorganizes following deafferentation. For example, recordings made in VPL in neonatal amputated rat pups that were mapped as adults showed clear evidence of functional reorganization whereby new hindlimb receptive fields appeared in deafferented VPL (Stojic et al., 1998). Following sectioning of peripheral forelimb afferents in adult monkeys, functional reorganization was observed in VPL that was as extensive as previously reported in SI cortex (Garraghty and Kaas, 1991). Digit removal in adult raccoon resulted in a similar reorganization in VPL where input from the neighboring digits was reported in the deafferented digit zone (Rasmusson, 1996a). One recurrent suggestion from these findings was that the reorganization in VPL that follows digit or forelimb amputation accounts for the reorganization observed in SI cortex following deafferentation. In the present study, direct evidence was provided that a shoulder responsive site in the presumptive former digit

territory in deafferented VPL conveyed that new shoulder input to the deafferented FBS over the same thalamocortical pathway that once relayed forepaw input to the FBS. Conversely, this same shoulder responsive site in VPL did not project to the original shoulder representation in SI.

While we and others suggest that the resulting SI reorganization that follows deafferentation depends on subcortical changes (Garraghty and Kaas, 1991; Li et al., 2013; Pearson et al., 2001; Rasmusson, 1996b; Stojic et al., 1998), this conclusion is not without exception (Darian-Smith and Gilbert, 1995). Previously we reported that following forelimb amputation, new input was first observed in FBS within 4 weeks after amputation and by 6 weeks, new shoulder responses could be recorded throughout most of the FBS (Pearson et al., 2003). We reasoned that, because of the significant longer evoked response latencies recorded in the FBS, the new shoulder responses in the FBS were relayed from the original shoulder representation in SI and/or from SII. To determine whether an axonal pathway linked the original shoulder cortex to the FBS, anatomical tracers were injected into each region, but a direct connection was not found (Pearson et al., 2001). As a follow up, thermal ablation of the original shoulder representation and/or SII failed to eliminate the new shoulder responses in the FBS, suggesting that cortical reorganization was very likely mediated at a subcortical level. This finding may be contrasted with the results of a study of reorganization in striate cortex in cat and monkey following bilateral retinal lesions. In that study, investigators found no evidence for reorganization in the thalamic relay nucleus (lateral geniculate) or in thalamocortical projections, but rather the resulting cortical reorganization was mediated by collaterals of long-range horizontal corticocortical connections (Darian-Smith and Gilbert, 1995).

3.2.2 – Thalamocortical projections (VPL to SI)—For new shoulder input to reach the FBS, we proposed that it was relayed from deafferented forepaw VPL that became responsive to shoulder input following amputation. Our electroanatomy data (see Figure 5) showed that a location in the presumptive D1/TH representation in VPL, now responsive to new shoulder input, projected to a shoulder-responsive site in SI, formerly associated with the representation of D1/TH. At the same time, neurons at that thalamic site could not be antidromically-activated by stimulating sites in the original shoulder representation or surrounding upper arm representation in SI.

In forelimb intact rats, stimulation of the forepaw and shoulder evoked responses in homotopic sites in SI. Similarly, stimulation of sites in forepaw and shoulder VPL evoked responses in homotopic sites in SI, although it is reported that thalamocortical axons from forepaw VPL terminate primarily at homotopic sites in SI but also send sparse projections to neighboring cortical barrels (Arnold et al., 2001). While we studied peripheral and thalamic projections only in forelimb intact rats, there is little evidence to support a change in the thalamocortical projection pattern in deafferented rodent (Keller and Carlson, 1999; Stojic et al., 1998; Verney et al., 1982), cat (McKinley and Kruger, 1988), raccoon (Rasmusson and Nance, 1986; Rasmusson, 1996b), and monkey (Darian-Smith and Gilbert, 1995). In neonatal rats, forelimb amputation results in new hindlimb input into deafferented forelimb cortex but when injections of tracer were made in VPL no differences were observed in the projection pathway between controls and deafferents (Stojic et al., 1998).

It is also possible that thalamocortical axons from shoulder sites in VPL give off collaterals to forelimb sites in VPL and/or sprout new connections to forepaw VPL after deafferentation, but our data does not address this possibility. In a previous thalamocortical study in barrel cortex, axons of intracellularly labeled neurons in VPL did not give off collaterals within VPL on their trajectory to barrel cortex, but axonal branching was observed as the axons passed through RTN (Arnold et al., 2001).

3.2.3 – Role(s) of CN in large-scale cortical reorganization—Our previous finding that CN did not play a role in large-scale cortical reorganization following forelimb amputation in young adult rats (Li et al., 2013) can be compared to studies in which forelimb amputation was carried out in neonatal rats (Lane et al., 1995). These investigators observed that, following neonatal amputation, new hindlimb afferents invaded the deafferented forelimb zone in CN and 40% of the recorded cells developed split receptive fields that included both the hindlimb and stump (Lane et al., 1995). However, when amputations were made in adult rats, only 2% of the CN neurons have split-receptive fields (Bowlus et al., 2003). In the present study in adult rats, it is possible that primary afferents from the shoulder invaded the deafferented forepaw zone in CN but were functionally unexpressed. Similar findings of a mismatch between the appearance of sprouted hindlimb afferents into CN and their functional expression have been reported (Rhoades et al., 1993); however, even at 30 weeks after amputation, few cells in the central zone in CN responded to input from the shoulder, and those were localized to the outer region bordering the forepaw zone (Li et al., 2013).

The failure to find evidence to support our prediction that CN reorganization provided the source of new input to VPL (Li et al., 2013) led us to use anatomical tracing and electroanatomy in the current study to reexamine cuneothalamic projection in forelimb intact rats. Our data show that cuneothalamic axons from the shoulder give off branches to the forepaw zone in VPL, but this input is insufficient to evoke shoulder responses in the forepaw VPL in forelimb intact rats. Nonetheless, afferent input from the shoulder CN is available and could provide a substrate for the expression of new shoulder input into forepaw VPL following forelimb amputation. One suggestion is that this input is under GABAergic modulatory control from the RTN and that forelimb amputation leads to the release of inhibition.

3.2.4 – Reticular nucleus (RTN)—Rat VPL has few intrinsic interneurons (Barbaresi et al., 1986; De Biasi et al., 1988) and therefore relies on its GABA innervation from the RTN (Harris and Hendrickson, 1987; Houser et al., 1980). RTN is somatotopically organized with the limb and trunk representations located in the dorsal-rostral-intermediate part, receives input from medial lemniscus and SI cortex, and projects topographically to VB (De Biasi et al., 1988; Deschenes et al., 1994; Shosaku et al., 1984; Shosaku, 1985; Shosaku, 1986). RTN is composed of a homogenous population of GABAergic neurons that project to VPL topographically, and is reciprocally connected by projections from VB (De Biasi et al., 1988; Pinault et al., 1995). RTN lesions increase receptive field size in VB (Lee et al., 1994a) while stimulation of RTN suppresses spontaneous activity and evoked discharges in VB neurons (Mushiake et al., 1984). Our previous data also confirm that RTN modulates

receptive field size of VPL neurons (Li et al., 2005). We identified a physiologically site in RTN that had a receptive field on the forepaw; a location having a similar receptive field on the forepaw was then identified in VPL. Stimulation in the forepaw VPL antidromically-activated a cell in the forepaw RTN. The site in RTN was then ablated by passing a current through the recording electrode; subsequently, the receptive field in VPL enlarged to include the arm and shoulder. We suggest that RTN imposes a similar modulation on cuneothalamic terminals originating from the shoulder region in CN that give off branches to the forepaw region. Following amputation, there is a likely release from inhibitory modulation onto cuneothalamic terminals that leads to the expression of new shoulder input in the deafferent VPL. This new shoulder input is then available to deafferented SI over the same cuneothalamic pathway that previously relayed forepaw input to the FBS.

3.3 Other comments

Present findings support the notion that VPL provides a substrate for delayed large-scale cortical reorganization in the FBS after forelimb amputation. We previously reported that new input from the shoulder was first observed in deafferented FBS 4 weeks after forelimb amputation (Pearson et al., 2003). New input had a longer evoked response latency following stimulation of the shoulder than the evoked response latency recorded in the original shoulder representation in SI (Pearson et al., 1999). One possible explanation for the longer evoked response latencies may relate to differences in transmission characteristics across synaptic junctions in VPL. In the present study, injections of tracer in physiologically identified shoulder or forepaw sites in CN produced dense labeling in their respective homotopic sites in VPL. In contrast, only sparse labeling was observed from the axonal side branches that coursed through non-homotopic forelimb or shoulder sites in VPL. Terminals found at these homotopic and nonhomotopic sites may have different synaptic linkages (Rowe, 2002a; Rowe, 2002b) such that contacts at non-homotopic sites are ineffective until some change occurs in the neighboring homotopic synapses (Merrill and Wall, 1972). The main terminals within homotopic sites in VPL most likely produce fast synaptic transmission onto thalamocortical projection neurons that in turn lead to concomitant short latency evoked responses in their target sites in SI. Conversely, the side branches are sparsely distributed in the non-homotopic sites and would necessitate temporal and possibly spatial summation to bring the VPL cell to spiking level. It is also possible that the axon terminals of CN neurons make synaptic connections at more distal sites on the dendrites of the VPL projection neurons in the non-homotopic regions. Together, temporal summation and site of termination could account for the reported 5-msec difference in evoked response latencies in original and new shoulder representations in SI that follow forelimb amputation.

We speculate that the new shoulder input to forelimb VPL is functionally weak and therefore requires less inhibitory control from the RTN to maintain suppression. Following deafferentation, the principal input from the forepaw is lost and the new shoulder input gradually gains strength over time. For delayed activation of the new shoulder input to become expressed in forelimb VPL, RTN must continue to exert some measure of GABAergic inhibition over VPL forepaw neurons immediately after deafferentation and for a period of time thereafter. For the case of new shoulder representation in the FBS, the inhibitory control must be maintained for 3 or more weeks after deafferentation, perhaps

because RTN neurons are modulated downstream from SI (Bourassa et al., 1995) or RTN projection neurons to VPL are not completely knocked out following deafferentation due to existence of prolonged auto-inhibition within RTN neurons (De Biasi et al., 1988). This may explain why ablation of RTN projection neurons leads to the immediate expansion of receptive fields in the forepaw VPL to include regions of the upper arm and shoulder (Li et al., 2005).

3.4 Mechanisms for delayed large-scale reorganization

The reorganization that occurs within the FBS is not immediate but is delayed for a period of weeks after forelimb amputation; in contrast, new shoulder input was observed in the former arm representation, which lies adjacent to the original shoulder representation in SI as early as 2 weeks post-amputation (Pearson et al., 2003). Cortical reorganization has been described as occurring in two (Calford and Tweedale, 1991; Cusick et al., 1990; Merzenich et al., 1983) or more stages (Churchill et al., 1998). In the first stage, new receptive fields are immediately revealed after deafferentation. Merzenich et al. (1983) transected the median nerve in adult monkey and mapped new receptive fields in the deafferented median nerve cortex immediately after nerve cut; however, much of former median nerve cortex remained unresponsive. By post-transection day 22 these investigators reported that the median nerve territory was completely reoccupied by new receptive field input from the surrounding ulnar and radial regions of the skin. Besides repopulating the deafferented median nerve territory, changes in receptive field topography were observed over the ensuing months. With protracted periods of reorganization lasting 11 or more months, post-amputation, a third stage of reorganization was described whereby further refinements in topography, sharpening of receptive fields, and an increase in the presence of non-cutaneous receptive fields was observed (Churchill et al., 1998).

The new receptive fields recorded immediately after deafferentation most likely result from the expression of preexisting subthreshold inputs that are under GABAergic control (Alloway and Burton, 1991; Hicks and Dykes, 1983; Li et al., 2002); furthermore, deafferentation has been shown to down-regulate $GABA_A$ receptors (Fuchs and Salazar, 1998; Wellman et al., 2002) and the down-regulation persists for months (Garraghty et al., 2006). However the second stage of reorganization may be under a different set of mechanisms since acetylcholine (Ach) depletion (Baskerville et al., 1997; Juliano et al., 1991; Webster et al., 1991) or blockage of NMDA receptors (Garraghty and Muja, 1996) prevents its occurrence. Our delayed large-scale reorganization results are most closely aligned with this second stage of reorganization, since we found no evidence of immediate reorganization occurring in the FBS post-amputation week 4 or in the entire deafferented forelimb territory before the second post-deafferented week (Pearson et al., 2003). We cannot rule out a role for ACh or NMDA receptors as mechanisms underlying delayed large-scale reorganization. Our results, first and foremost, provide evidence that new shoulder input in deafferented SI originates from forepaw VPL and this new shoulder input is relayed to the deafferented FBS over the former forepaw pathway. Whether new shoulder input appears immediately in the deafferented forepaw VPL was not examined nor were other possible mechanisms. We, and others, have shown that RTN modulates receptive field size of VPL forepaw neurons and that RTN provides GABAergic input onto VPL neurons (Lee et

al., 1994b; Li et al., 2005). VPL neurons become hyperactive 1 to 2 weeks following transection of the spinothalamic tract by recruitment of NMDA receptors (Koyama et al., 1993) and these receptors are reported to mediate synaptic transmission in both VPL and RTN (Liu, 1997). It is interesting to note that following nerve transection in monkey, $GABA_A$ receptor binding is reduced in layer IV of SI within hours of nerve transection (Wellman et al., 2002) and remains reduced at least 2 months after transection (Garraghty et al., 2006) while NMDA receptor binding shows little change throughout the 2 months. It may be that the resulting GABA down-regulation in both VPL and SI provides a permissive environment for the activation of NMDA receptors and possibly plays a role in modulating ACh as well. If GABA down-regulation were compensated for following deafferentation, then it may be that neither stage of reorganization will be manifested. We therefore cannot rule out the possibility that GABAergic modulation may also play an important role in delayed cortical reorganization.

Summary—In this study, we examined the organization and reorganization of VPL in adult rats and provide evidence that new shoulder input becomes expressed in the deafferented forepaw VPL. This new shoulder input is relayed to deafferented forepaw SI and provides a substrate for large-scale cortical reorganization. In addition, forepaw VPL receives projection from shoulder responsive sites in CN, which are likely subthreshold and not expressed until after forelimb amputation. We speculate that the expression of new shoulder input in forepaw VPL that follows deafferentation results from a down-regulation of GABA input from RTN that in turn elevates subthreshold shoulder input from CN.

4. Experimental procedure

4.1. Animals

A total of 29 adult rats was used to examine the substrate underlying large-scale cortical reorganization that results after forelimb amputation. The body surface was mapped in rat VPL by recording receptive fields using carbon fiber electrodes in forelimb intact rats (n=8) and in forelimb amputees (n=5) 7–24 weeks after amputation. The pattern of projection from forelimb and shoulder periphery to SI cortex was examined in forelimb intact rats (n=2), and the projection from forepaw and shoulder zones in VPL to SI was studied in another 3 rats. Projections from deafferented forepaw VPL to SI were examined in 2 rats. The cuneothalamic pathway was studied using an anatomical tracer in 5 rats and by using microstimulation and recording technique in 4 rats. These experiments conformed to the Principles of Laboratory Animal Care (NIH publication No. 86–23, revised 1985) and were approved by the Animal Care and Use Committee, University of Tennessee Health Science Center.

4.2. Forelimb amputation

Amputation of the forelimb in young adult rats was previously described (Li et al., 2013; Pearson et al., 1999). Briefly, under aseptic conditions, rats between 7 and 8 weeks of age were anesthetized with Nembutal (35 mg/kg, i.p.), the skin and external shoulder muscles were reflected around the humerus, and the forelimb was amputated at the glenno-humeral joint. Surgical sutures (000) were used to ligate the forelimb nerves, and the brachial artery

was cauterized in the region of the brachial plexus. The skin flap surrounding the wound was closed using surgical sutures, and bupivacaine (0.7%) was topically applied to the wound tissue prior to closure for local analgesia. Immediately following amputation, animals were given a sedative (buprenorphine, 0.05–0.1 mg/kg i.m.) for the first 48 postoperative hours for systemic analgesic effects. An antibiotic, Crystiben (penicillin G, 30,000 IU/kg, i.m., BID) was also given at the end of the surgery. Rats were monitored until they recovered from anesthesia and thereafter monitored daily. Rats were then returned to their home cage with ad libitum access to food and water until undergoing physiological mapping.

4.3. Physiological mapping and map reconstruction

A brief description of physiological mapping methods is presented here; for a more detailed description see (Pearson et al., 2003; Waters et al., 1995). Rats were weighed and anesthetized with Ketamine/Xylazine (100 mg/kg) and supplemented with a 10% dosage to maintain areflexia. The hair on the head, neck, and forelimb was shaved. Body temperature was maintained within the range of 36°–38°C by placing the rat on a water-circulating heating pad. Sterile saline (0.9%) was administered (i.p.) at hourly intervals for fluid maintenance. A stereotaxic frame was used to secure the animal's head. A slit was made in the skin overlying the scalp, the bone overlying the presumptive sensorimotor cortex was removed, and the dura was opened and retracted over the bone. A recording chamber formed from dental cement was placed around the opened skull, and the cortical surface was covered with silicon oil (10,000 cs) to prevent drying. A digital image of the brain surface was taken, viewed on a computer screen, and used to mark the surface position of electrode penetrations.

Single and multiunit responses were recorded in SI and VPL with a carbon fiber electrode attached to a Narishige (Canberra-type) microdrive. The amplified signal was fed into a storage oscilloscope, audio monitor, and data storage unit. Cutaneous receptive fields were examined using a wooden probe or fine-tipped brush. Receptive fields were recorded at a depth of 700 μm in SI or at 200-μm intervals along a thalamic penetration; receptive fields were drawn on a map of the body surface. Sites over the stump were examined by using a brush to lightly stimulate the skin surface, and every effort was made to separate cutaneous responses from the overlying skin from the deeper responses evoked from the stump. Electrolytic lesions (cathodal current, 5μA × 10 sec) were made at selected sites of interest in SI or in VPL.

At the end of mapping, rats were given a lethal dose of Nembutal and perfused intracardially with 0.9% saline followed by 4% paraformaldehyde as previously described (Li et al., 2012; Li et al., 2013; Waters et al., 1995). In experiments where the cortex alone was studied, the brain was removed from the skull, blocked, and placed between a pair of Plexiglas plates and flattened overnight in perfusion solution. The following day, the tissue was sectioned along a tangential plane on a Vibratome at 100-micron thickness and reacted with cytochrome oxidase (CO). In experiments where both cortex and thalamus were studied in the same animal, the brain was blocked on a coronal plane at the approximate location of the forearm representation. The anterior part of the brain was flattened as described above and cut on a tangential plane, while the posterior part, containing VPL, was sectioned at 100-

micron thickness along the coronal plane. Tissues from both cortex and thalamus were then stained with CO, mounted on glass slides, and cover-slipped. Sections were photographed on a digital camera or scanned using a high-resolution digital scanner, Whole Slide Imaging (WSI) System (Aperio).

Electrode penetrations and receptive field(s) recorded along penetrations were extrapolated from the lesion data or from coagulated blood along a penetration and plotted in relationship to the underlying morphological map. We attempted to restrict our mapping of VPL to a narrow region that contained the entire limb and trunk representation that passed through a single coronal slice that enabled us to align sections from different animals with minimal distortion.

To obtain a standard map of the ventrobasal complex (VPM, VPL, RTN), we used a best-fit line approach to generate a composite outline. Brain sections from the study animals were reconstructed from a scanned image, and a circle was placed at the approximate center of each section. The sections were then superimposed upon one another at the center location, and the overall size of the map was adjusted and aligned to produce a close overlap between the section outlines. A protractor aligned at the center location was then placed over the superimposed section outlines. Radial lines in 4^0- increments were then drawn, and the radial distance from the center location was measured as the radial line passed through each section drawing. The averaged distance of the individual sections was then used as a data point to represent that radial location. The resulting data points were then connected, smoothed, and used to produce a best-fit line.

4.4. Pathway mapping

4.4.1 – Forelimb and shoulder projection to SI cortex in forelimb intact rats—In 2 rats, digit, wrist, arm, and shoulder representations in SI cortex were mapped using mechanical stimulation. Once a receptive field was identified, a probe, consisting of a pair of silver leads, was used to deliver stimulus pulses (1-ms duration, 1 Hz, 1.5 × threshold amplitude) to the skin surface and evoked responses were recorded in SI. The maximum stimulation current was always less than 150 μA, which was below the level that produced visible muscle contractions. A site on the forepaw (e.g., D3v) and shoulder skin surface was selected to stimulate, and input was examined at each of the previously identified forelimb and shoulder receptive field sites in SI. Single, averaged (10 consecutive stimulations), and buffer responses for 10 consecutive stimulations were collected, stored, and analyzed on a computer using IGOR Pro (Wavemetrics).

4.4.2 – Forepaw and shoulder projections to VPL and projections from forepaw and shoulder zones in VPL to forepaw and shoulder SI cortex in forelimb intact rats—In 3 forelimb intact rats, mechanical stimulation was used to physiologically identify forepaw and shoulder receptive field sites in VPL. Matching receptive fields sites in the original shoulder and FBS in SI cortex were then physiologically identified. The recording electrode in VPL was used to deliver single pulse microstimulation (1-ms duration, 1 Hz, <50 μA stimulus amplitude) to the previously identified forepaw and shoulder sites in VPL and evoked responses were examined at original shoulder and FBS

sites in SI. Conversely, the cortical electrode could be used to deliver microstimulation in an effort to antidromically-activate responses in VPL. Antidromic activation was defined in this study by high frequency firing response and invariant latency; the collision test was not used (Waters et al., 1982). A stimulating probe was also used to examine peripheral input from the forepaw and shoulder to each zone in VPL.

4.4.3 – VPL to SI projections in forelimb amputees—In 2 forelimb-amputated rats, the projection from the presumptive forepaw zone in VPL to the deafferented FBS was examined using extracellular recording and microstimulation. A carbon fiber electrode was inserted into a presumptive former digit location in VPL where new input from the shoulder was recorded. A second electrode was next inserted into the FBS that now received input from the shoulder. Microstimulation was then delivered to the cortical electrode in an effort to antidromically activate cells in VPL. We defined a direct projection as those cases where a cell in VPL was antidromically-activated by microstimulation in SI. An electrode was also inserted into the original shoulder representation in SI to test for antidromic activation in VPL.

4.5. Cuneothalamic tracing

4.5.1. – Anatomical tracing—BDA was iontophoresed (7-min injection time, +1-μA injection current, 7-sec duty cycle) into a physiologically defined region in the shoulder or forepaw representation in CN in forelimb intact rats (n=5). A carbon fiber electrode was initially used to identify a receptive field in the forepaw or shoulder representation. The electrode was replaced with a glass pipette containing a 2% solution of BDA in 1M K-Acetate, and BDA was iontophoresed using a precision current source (Midgard). The pipette remained in the tissue for 2 min before withdrawal. Following the injection, the opening in the brainstem was closed with dental cement and the overlying skin was sutured. Postoperative care included administering an antibiotic, Crystiben (penicillin G, 30,000 IU/kg, i.m.), and a sedative (buprenorphine, 0.05–0.1 mg/kg i.m.). Following a 5–7 day survival, rats were administered a lethal dose of Nembutal (100 mg/kg, i.m.) and transcardially perfused with 0.9% saline followed by chilled 4% paraformaldehyde in 0.3 M sodium phosphate– buffered saline (NaPBS, pH 7.4, 21°C). The brainstem was removed and blocked. Tissue was fixed in 4% paraformaldehyde at 4°C and refrigerated overnight. The following day, tissue was sectioned along a sagittal plane at 100-μm thickness using a Vibratome. Sections were incubated in ABC Elite (1:200 in 0.01 M KPBS) for 4 h and rinsed (3 × 10 min) in 0.01 M KPBS (pH 7.4, 21°C). Tissue was reacted with a 0.05% 3, 3′ DAB-KPBS intensified with a solution of nickel ammonium sulfate (1%) and hydrogen peroxide (30%). Sections were rinsed (2 × 5 min) in 0.01 M KPBS, counterstained with CO, and mounted on gelatin-coated slides.

4.5.2. – Electroanatomy—Microstimulation was used to examine the projection between forelimb and shoulder sites in CN and VPL in forelimb intact rats (n=4). Animal preparation and physiological recording and mapping were identical to the above description. A carbon fiber recording electrode was inserted into a physiologically identified location in the forepaw or shoulder zone in VPL. A second electrode was then inserted into the shoulder representation in CN. The thalamic electrode was then used to deliver single pulses (1.0 ms,

1 Hz, ISI, maximum current 30 μA). Whenever a CN neuron was activated, its mode of activation was determined. The response was classified as antidromic when the neuron responded with a constant latency to threshold stimulation and invariant latency (≤0.1 ms) to rapid stimulation (<0.1 Hz) at 2 × threshold (Waters et al., 1982).

In 2 additional rats, the extracellular recording electrode in CN was replaced by an intracellular electrode containing 2% biocytin and was inserted into the brainstem at the approximate location of previous extracellular electrode. The electrode was used to record the receptive field of an impaled cell and to label the cell for subsequent identification of cell type and recording location (Arnold et al., 2001; Li and Waters, 1996; Li et al., 2002). Evoked responses were fed through an A/D converter and analyzed using IgorPro (Wavemetrics, Inc.) software system. Recordings were also stored on VHS tape using a Neurocorder (Model DR-384) for subsequent off-line analysis (Waters et al., 1995; Wong-Riley, 1979; Wong-Riley and Welt, 1980). Intracellularly labeled neurons were reacted with DAB and the background tissue was countered-stained with CO, as previously described (Arnold et al., 2001; Li and Waters, 1996; Li et al., 2002).

Acknowledgments

Supported by National Institutes of Health/National Institute of Neurological Disorders and Stroke; grant number: NS-055236. This research was supported by NIH grant AA-013437-01 to R.S.W. The authors thank Ms.M. Waters for editing the manuscript. We thank Dr. Oleg Favorov for his valuable comments on the manuscript. We thank Dr. A. Kulkarni for technical assistance with the Whole Slide Imaging (WSI) system.

Literature

Alloway KD, Burton H. Differential effects of GABA and bicuculline on rapidly- and slowly-adapting neurons in primary somatosensory cortex of primates. Exp Brain Res. 1991; 85:598–610. [PubMed: 1655509]

Alloway KD, Aaron GB. Adaptive changes in the somatotopic properties of individual thalamic neurons immediately following microlesions in connected regions of the nucleus cuneatus. Synapse. 1996; 22:1–14. [PubMed: 8822473]

Angel A, Clarke KA. Fine somatotopic representation of the forelimb area of the ventrobasal thalamus of the albino rat. J Physiol. 1973; 233:43P–44P.

Angel A, Clarke KA. An analysis of the representation of the forelimb in the ventrobasal thalamic complex of the albino rat. J Physiol. 1975; 249:399–423. [PubMed: 1177098]

Arnold PB, Li CX, Waters RS. Thalamocortical arbors extend beyond single cortical barrels: an in vivo intracellular tracing study in rat. Exp Brain Res. 2001; 136:152–68. [PubMed: 11206278]

Barbaresi P, Spreafico R, Frassoni C, Rustioni A. GABAergic neurons are present in the dorsal column nuclei but not in the ventroposterior complex of rats. Brain Res. 1986; 382:305–26. [PubMed: 2428443]

Baskerville KA, Schweitzer JB, Herron P. Effects of cholinergic depletion on experience-dependent plasticity in the cortex of the rat. Neuroscience. 1997; 80:1159–69. [PubMed: 9284068]

Belford GR, Killackey HP. Anatomical correlates of the forelimb in the ventrobasal complex and the cuneate nucleus of the neonatal rat. Brain Res. 1978; 158:450–5. [PubMed: 81706]

Bourassa J, Pinault D, Deschenes M. Corticothalamic projections from the cortical barrel field to the somatosensory thalamus in rats: a single-fibre study using biocytin as an anterograde tracer. Eur J Neurosci. 1995; 7:19–30. [PubMed: 7711933]

Bowlus TH, Lane RD, Stojic AS, Johnston M, Pluto CP, Chan M, Chiaia NL, Rhoades RW. Comparison of reorganization ofthe somatosensory system in rats that sustained forelimb removal as neonates and as adults. J Comp Neurol. 2003; 465:335–48. [PubMed: 12966559]

Calford MB, Tweedale R. Acute changes in cutaneous receptive fields in primary somatosensory cortex after digit denervation in adult flying fox. J Neurophysiol. 1991; 65:178–87. [PubMed: 2016636]

Churchill JD, Muja N, Myers WA, Besheer J, Garraghty PE. Somatotopic consolidation: a third phase of reorganization after peripheral nerve injury in adult squirrel monkeys. Exp Brain Res. 1998; 118:189–96. [PubMed: 9547087]

Crockett DP, Maslany S, Harris SL, Egger MD. Enhanced cytochrome-oxidase staining of the cuneate nucleus in the rat reveals a modifiable somatotopic map. Brain Res. 1993; 612:41–55. [PubMed: 7687194]

Cusick CG, Wall JT, Whiting JH Jr. Wiley RG. Temporal progression of cortical reorganization following nerve injury. Brain Res. 1990; 537:355–8. [PubMed: 2085786]

Darian-Smith C, Gilbert CD. Topographic reorganization in the striate cortex of the adult cat and monkey is cortically mediated. J Neurosci. 1995; 15:1631–47. [PubMed: 7891124]

Davidson N. The projection of afferent pathways on the thalamus of the rat. J Comp Neurol. 1965; 124:377–90. [PubMed: 5861719]

De Biasi S, Frassoni C, Spreafico R. The intrinsic organization of the ventroposterolateral nucleus and related reticular thalamic nucleus of the rat: a double-labeling ultrastructural investigation with gamma- aminobutyric acid immunogold staining and lectin-conjugated horseradish peroxidase. Somatosens Res. 1988; 5:187–203. [PubMed: 3282295]

Deschenes M, Bourassa J, Pinault D. Corticothalamic projections from layer V cells in rat are collaterals oflong-range corticofugal axons. Brain Res. 1994; 664:215–9. [PubMed: 7895031]

Emmers R. Organization of the First and the Second Somesthetic Regions (Si and Sii) in the Rat Thalamus. J Comp Neurol. 1965; 124:215–27. [PubMed: 14330741]

Francis JT, Xu S, Chapin JK. Proprioceptive and cutaneous representations in the rat ventral posterolateral thalamus. J Neurophysiol. 2008; 99:2291–304. [PubMed: 18287546]

Fuchs JL, Salazar E. Effects of whisker trimming on GABA(A) receptor binding in the barrel cortex of developing and adult rats. J Comp Neurol. 1998; 395:209–16. [PubMed: 9603373]

Garraghty PE, Kaas JH. Functional reorganization in adult monkey thalamus after peripheral nerve injury. Neuroreport. 1991; 2:747–50. [PubMed: 1793816]

Garraghty PE, Muja N. NMDA receptors and plasticity in adult primate somatosensory cortex. J Comp Neurol. 1996; 367:319–26. [PubMed: 8708013]

Garraghty PE, Arnold LL, Wellman CL, Mowery TM. Receptor autoradiographic correlates of deafferentation-induced reorganization in adult primate somatosensory cortex. J Comp Neurol. 2006; 497:636–45. [PubMed: 16739196]

Harris RM, Hendrickson AE. Local circuit neurons in the ratventrobasal thalamus--a GABA immunocytochemical study. Neuroscience. 1987; 21:229–36. [PubMed: 3299139]

Hicks TP, Dykes RW. Receptive field size for certain neurons in primary somatosensory cortex is determined by GABA-mediated intracortical inhibition. Brain Res. 1983; 274:160–4. [PubMed: 6137268]

Houser CR, Vaughn JE, Barber RP, Roberts E. GABA neurons are the major cell type of the nucleus reticularis thalami. Brain Res. 1980; 200:341–54. [PubMed: 7417821]

Jaw FS, Kao YC, Chen CP, Lee CY, Chen YY. High-fidelity evoked potential for mapping the rat tail in thalamus. Neuroscience. 2008; 155:277–82. [PubMed: 18597944]

Juliano SL, Ma W, Eslin D. Cholinergic depletion prevents expansion of topographic maps in somatosensory cortex. Proc Natl Acad Sci USA. 1991; 88:7804.

Keller A, Carlson GC. Neonatal whisker clipping alters intracortical, but not thalamocortical projections, in rat barrel cortex. J Comp Neurol. 1999; 412:83–94. [PubMed: 10440711]

Koyama S, Katayama Y, Maejima S, Hirayama T, Fujii M, Tsubokawa T. Thalamic neuronal hyperactivity following transection of the spinothalamic tract in the cat: involvement ofN-methyl-D-aspartate receptor. Brain Res. 1993; 612:345–50. [PubMed: 8101136]

Lane RD, Bennett-Clarke CA, Chiaia NL, Killackey HP, Rhoades RW. Lesion-induced reorganization in the brainstem is not completely expressed in somatosensory cortex. Proc Natl Acad Sci USA. 1995; 92:4264–8. [PubMed: 7753794]

Lane RD, Pluto CP, Kenmuir CL, Chiaia NL, Mooney RD. Does reorganization in the cuneate nucleus following neonatal forelimb amputation influence development of anomalous circuits within the somatosensory cortex? J Neurophysiol. 2008; 99:866–75. [PubMed: 18032566]

Lee SM, Friedberg MH, Ebner FF. The role of GABA-mediated inhibition in the rat ventral posterior medial thalamus. I. Assessment of receptive field changes following thalamic reticular nucleus lesions. J Neurophysiol. 1994a; 71:1702–15. [PubMed: 8064343]

Lee SM, Friedberg MH, Ebner FF. The role of GABA-mediated inhibition in the ratventral posterior medial thalamus. II. Differential effects of GABAA and GABAB receptor antagonists on responses ofVPM neurons. J Neurophysiol. 1994b; 71:1716–26. [PubMed: 8064344]

Li CX, Waters RS. In vivo intracellular recording and labeling of neurons in the forepawbarrel subfield (FBS) of rat somatosensory cortex: possible physiological and morphological substrates for reorganization. Neuroreport. 1996; 7:2261–72. [PubMed: 8951838]

Li CX, Callaway JC, Waters RS. Removal of GABAergic inhibition alters subthreshold input in neurons in forepaw barrel subfield (FBS) in rat first somatosensory cortex (SI) after digit stimulation. Exp Brain Res. 2002; 145:411–28. [PubMed: 12172653]

Li, CX, Chappell, TD, Waters, RS. 2005 Neuroscience Meeting Planner. Society for Neuroscience; Washington, DC: 2005. Possible roles ofThalamic Reticular Nucleus and Cuneate Nucleus in Large-Scale Cortical Reorganization.. Program No. 173.7 2005. Online

Li CX, Yang Q, Waters RS. Functional and structural organization of the forelimb representation in cuneate nucleus in rat. Brain Res. 2012; 1468:11–28. [PubMed: 22800965]

Li CX, Yang Q, Vemulapalli S, Waters RS. Forelimb amputation-induced reorganization in the cuneate nucleus (CN) is not reflected in large-scale reorganization in rat forepaw barrel subfield cortex (FBS). Brain Res. 2013; 1526:26–43. [PubMed: 23810455]

Liu XB. Subcellular distribution ofAMPA and NMDA receptor subunit immunoreactivity in ventral posterior and reticular nuclei of rat and cat thalamus. J Comp Neurol. 1997; 388:587–602. [PubMed: 9388018]

Maslany S, Crockett DP, Egger MD. Somatotopic organization ofthe cuneate nucleus in the rat: transganglionic labelling with WGA-HRP. Brain Res. 1990; 507:164–7. [PubMed: 1689203]

McKinley PA, Kruger L. Nonoverlapping thalamocortical connections to normal and deprived primary somatosensory cortex for similar forelimb receptive fields in chronic spinal cats. Somatosens Res. 1988; 5:311–23. [PubMed: 3381041]

Merrill EG, Wall PD. Factors forming the edge of a receptive field: the presence of relatively ineffective afferentterminals. J Physiol. 1972; 226:825–46. [PubMed: 4637631]

Merzenich MM, Kaas JH, Wall JT, Sur M, Nelson RJ, Felleman DJ. Progression of change following median nerve section in the cortical representation of the hand in areas 3b and 1 in adult owl and squirrel monkeys. Neuroscience. 1983; 10:639–65. [PubMed: 6646426]

Mushiake S, Shosaku A, Kayama Y. Inhibition of thalamic ventrobasal complex neurons by glutamate infusion into the thalamic reticular nucleus in rats. J Neurosci Res. 1984; 12:93–100. [PubMed: 6148426]

Nord SG. Somatotopic organization in the spinal trigeminal nucleus, the dorsal column nuclei and related structures in the rat. J Comp Neurol. 1967; 130:343–56. [PubMed: 6052603]

Pearson PP, Li CX, Waters RS. Effects oflarge-scale limb deafferentation on the morphological and physiological organization of the forepaw barrel subfield (FBS) in somatosensory cortex (SI) in adult and neonatal rats. Exp Brain Res. 1999; 128:315–31. [PubMed: 10501804]

Pearson PP, Arnold PB, Oladehin A, Li CX, Waters RS. Large-scale cortical reorganization following forelimb deafferentation in rat does not involve plasticity of intracortical connections. Exp Brain Res. 2001; 138:8–25. [PubMed: 11374086]

Pearson PP, Li CX, Chappell TD, Waters RS. Delayed reorganization of the shoulder representation in forepawbarrel subfield (FBS) in first somatosensory cortex (SI) following forelimb deafferentation in adult rats. Exp Brain Res. 2003; 153:100–12. [PubMed: 12955377]

Pinault D, Bourassa J, Deschenes M. The axonal arborization of single thalamic reticular neurons in the somatosensory thalamus of the rat. Eur J Neurosci. 1995; 7:31–40. [PubMed: 7711934]

Rasmusson D. Changes in the organization of the ventroposterior lateral thalamic nucleus after digit removal in adult raccoon. J Comp Neurol. 1996a; 364:92–103. [PubMed: 8789278]

Rasmusson DD, Nance DM. Non-overlapping thalamocortical projections for separate forepaw digits before and after cortical reorganization in the raccoon. Brain Res Bull. 1986; 16:399–406. [PubMed: 3011221]

Rasmusson DD. Changes in the response properties of neurons in the ventroposterior lateral thalamic nucleus of the raccoon after peripheral deafferentation. J Neurophysiol. 1996b; 75:2441–50. [PubMed: 8793755]

Rhoades RW, Wall JT, Chiaia NL, Bennett-Clarke CA, Killackey HP. Anatomical and functional changes in the organization of the cuneate nucleus of adult rats after fetal forelimb amputation. J Neurosci. 1993; 13:1106–19. [PubMed: 7680066]

Rowe MJ. The synaptic linkage for tactile and kinaesthetic inputs to the dorsal column nuclei. Adv Exp Med Biol. 2002a; 508:47–55. [PubMed: 12171144]

Rowe MJ. Synaptic transmission between single tactile and kinaesthetic sensory nerve fibers and their central target neurones. Behav Brain Res. 2002b; 135:197–212. [PubMed: 12356451]

Shosaku A, Kayama Y, Sumitomo I. Somatotopic organization in the rat thalamic reticular nucleus. Brain Res. 1984; 311:57–63. [PubMed: 6386105]

Shosaku A. A comparison of receptive field properties ofvibrissa neurons between the rat thalamic reticular and ventro-basal nuclei. Brain Res. 1985; 347:36–40. [PubMed: 4052804]

Shosaku A. Cross-correlation analysis of a recurrent inhibitory circuit in the rat thalamus. J Neurophysiol. 1986; 55:1030–43. [PubMed: 3711965]

Stojic AS, Lane RD, Killackey HP, Qadri BA, Rhoades RW. Thalamocortical and intracortical projections to the forelimb-stump SI representation of rats that sustained neonatal forelimb removal. J Comp Neurol. 1998; 401:187–204. [PubMed: 9822148]

Verley R, Onnen I. Somatotopic organization of the tactile thalamus in normal adult and developing mice and in adult mice dewhiskered since birth. Exp Neurol. 1981; 72:462–74. [PubMed: 7238702]

Verney C, Farkas-Bargeton E, Verley R. Reorganization of thalamo-cortical connections in mice dewhiskered since birth. Neurosci Lett. 1982; 32:265–70. [PubMed: 7177490]

Wall PD, Egger MD. Formation of new connexions in adult rat brains after partial deafferentation. Nature. 1971; 232:542–5. [PubMed: 4328622]

Waters RS, Favorov O, Asanuma H. Physiological properties and pattern of projection of cortico-cortical connections from the anterior bank of the ansate sulcus to the motor cortex, area 4 gamma, in the cat. Exp Brain Res. 1982; 46:403–12. [PubMed: 7095046]

Waters RS, Li CX, McCandlish CA. Relationship between the organization of the forepaw barrel subfield and the representation of the forepaw in layer IV of rat somatosensory cortex. Exp Brain Res. 1995; 103:183–97. [PubMed: 7789426]

Webster HH, Hanisch UK, Dykes RW, Biesold D. Basal forebrain lesions with or without reserpine injection inhibit cortical reorganization in rat hindpaw primary somatosensory cortex following sciatic nerve section. Somatosens Mot Res. 1991; 8:327–46. [PubMed: 1808975]

Wellman CL, Arnold LL, Garman EE, Garraghty PE. Acute reductions in GABAA receptor binding in layer IV of adult primate somatosensory cortex after peripheral nerve injury. Brain Res. 2002; 954:68–72. [PubMed: 12393234]

Wong-Riley M. Changes in the visual system of monocularly sutured or enucleated cats demonstrable with cytochrome oxidase histochemistry. Brain Res. 1979; 171:11–28. [PubMed: 223730]

Wong-Riley MT, Welt C. Histochemical changes in cytochrome oxidase of cortical barrels after vibrissal removal in neonatal and adult mice. Proc Natl AcadSciUSA. 1980; 77:2333–7.

highlights

- We describe the somatotopic organization in rat ventral posterior lateral (VPL) thalamic nucleus.
- We report the subsequent reorganization in rat forepaw VPL following forelimb amputation.
- Through mapping, we show that reorganized input in VPL is relayed to deafferented forepaw cortex.
- Cuneate nucleus provides latent forepaw input to VPL that is expressed only after deafferentation.
- VPL is a substrate for delayed large-scale cortical reorganization following amputation.

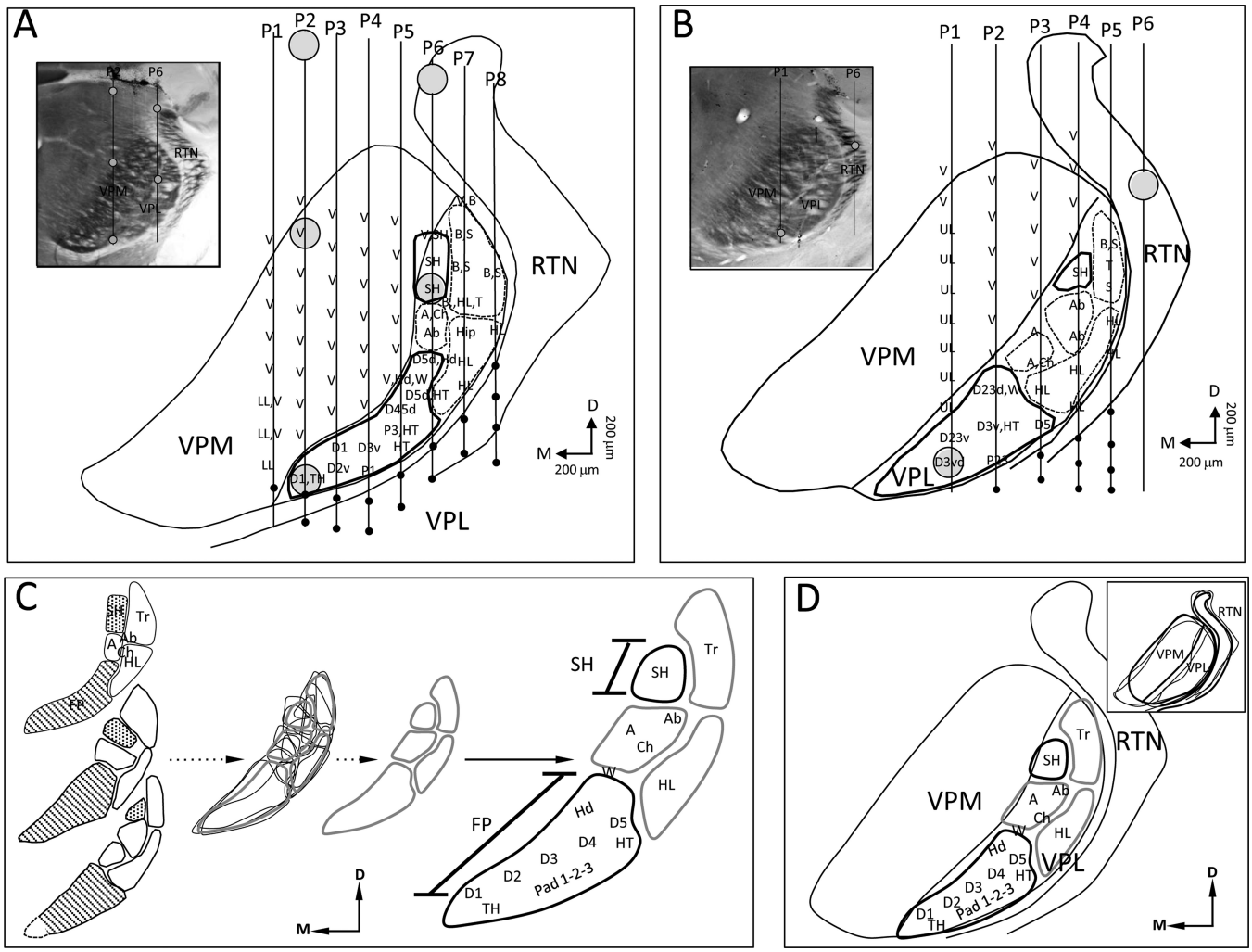

Fig. 1.

Photomicrographs, reconstructed line drawings, and interpretative summary of the organization of VPL in forelimb intact adult rats. **A:** Line drawing reconstruction showing a row of 8 electrode penetrations that passed through VPM, VPL, and/or RTN in 1 rat. Electrode penetrations nos. P2–P6 recorded receptive fields on the forepaw in the ventral part of the penetrations. P6 also recorded receptive fields on the shoulder upon superficial entry into VPL. Forepaw and shoulder regions are enclosed with heavy black lines; arm, trunk, and hindlimb zones are outlined with dashed lines. Lesions are indicated with large circles. Inset shows a photomicrograph of a CO-stained coronal section corresponding to the line drawing; lesions are shown with open circles in P2 and P6. **B:** Line drawing reconstruction showing a row of 6 electrode penetrations that passed through VPM, VPL, and/or RTN in another rat. In this example, only 3 electrode penetrations passed through the forepaw region and a separate penetration passed through the shoulder. Inset shows a CO-stained section through the recording area; lesions shown with open circles. **C:** Forepaw, arm, shoulder, trunk, and hindlimb zones from 3 rats, which were completely mapped, are aligned and superimposed upon one another and a best fit was drawn to produce a standard zone map shown at right. Note the dotted line added to the reconstruction in the lower

drawing (from Fig. 1B) to account for the presumptive location of the D1 representation. **D:** Similarly, VPM, VPL, and RTN were aligned (inset) from these 3 rats and a best fit was drawn to produce a standardized map. The zone maps from "C" were fitted into VPL showing our interpretation of somatotopic organization of the body map in VPL. Receptive field nomenclature: A = arm; Ab = abdomen; B = back; Ch = chest; FP = forepaw; Hip = hip; HL = hindlimb; LL = lower lip; S = side; SH = shoulder; T = tail; Tr = trunk; UL = upper lip; V = vibrissae; W = wrist. Sub-nomenclature for the forepaw: D = digit; 1-5 = digit number; d = dorsal; v = ventral; P = pad; TH = thenar pad; HT = hypothenar pad; Hd = dorsal hand.

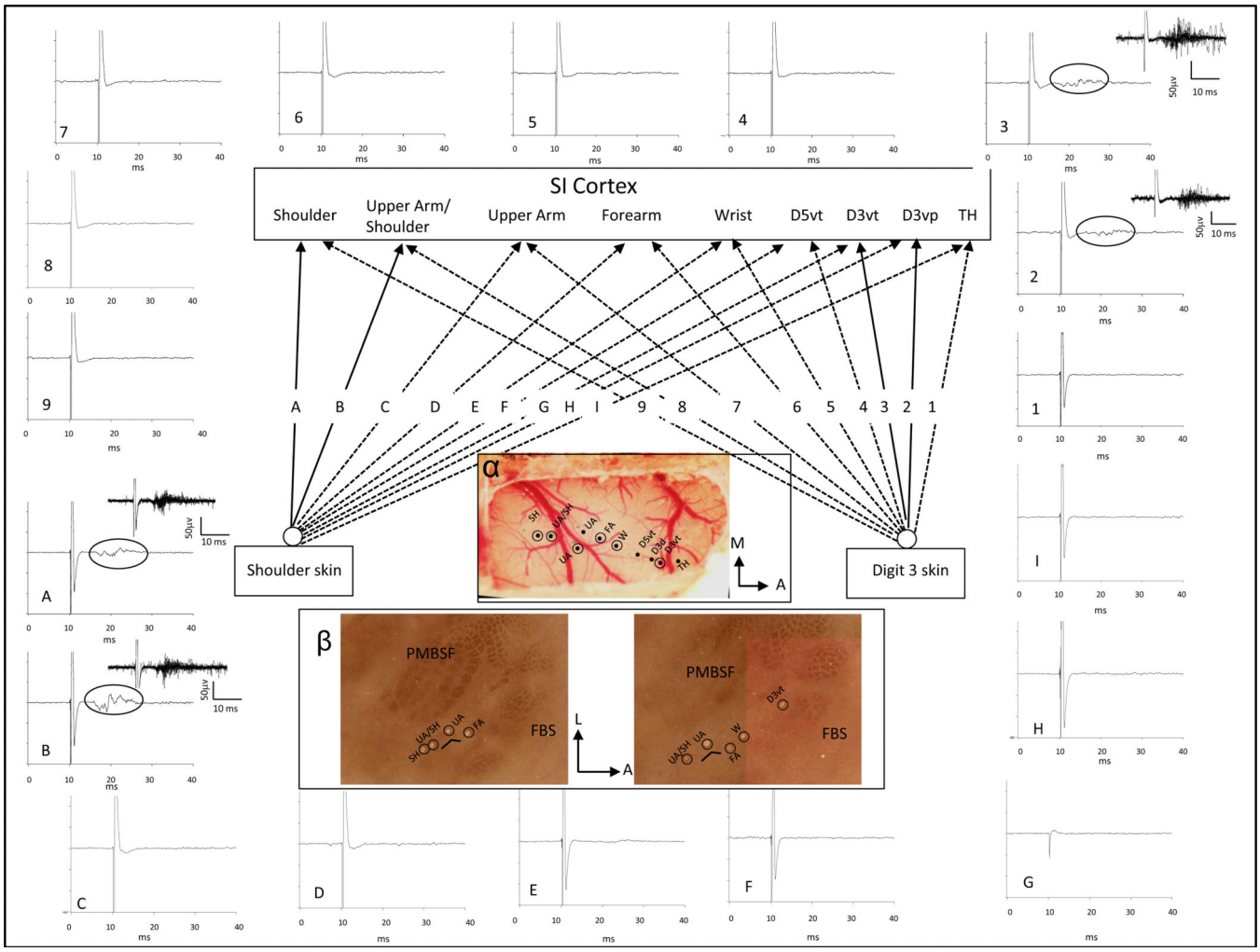

Fig. 2.

Pattern of projection from digit (nos. 1–9) and shoulder (letters A–I) to somatosensory cortex (SI) in 1 forelimb intact rat. SI was mapped using mechanical stimulation and sites were found that were responsive to input from thenar pad (TH), D3 ventral proximal (D3vp), D3 ventral tip (D3vt), D5 ventral tip (D5vt), wrist (W), forearm (FA), upper arm (UA), upper arm/shoulder, and shoulder (SH). A stimulating probe was placed on D3vt and single pulses (1-ms duration, 1 Hz) were delivered to the digit skin and recordings were made at each of the previous mapped sites in SI. Evoked responses were recorded only in the D3 cortical sites, and this is indicated by the solid lines and represented by nos. 2 and 3; no evoked responses were recorded at any of the other cortical sites at 3 × threshold, and this is indicated with the dashed lines. Averaged traces for 10 stimulations are displayed around the perimeter of the figure that correspond to each of the recording sites (1–9). Note that evoked responses were only observed in the D3 recording sites in SI and these are highlighted by ovals in the trace; insets show evoked response buffers for 10 consecutive stimulations. The stimulating probe was then placed on the shoulder and each site in SI was retested for evoked responses. Stimulation of the shoulder evoked responses only in the shoulder and upper arm/shoulder overlap region in SI. This is shown by solid lines represented by “A”

and “B”. Response records “A” and “B” are shown at the periphery along with traces (“C” through “I”) that did not show evoked responses. Ovals indicate evoked response in traces “A” and “B” and insets show evoked response buffers for 10 stimulations. **α:** Surface view of the cortex showing the electrode point of entry for each of the recording sites in SI; penetrations where lesions were made are shown with open circles. **β:** CO-stained flattened sections through SI showing the recording sites in the SI barrel cortex. Locations of lesions are shown by ovals.

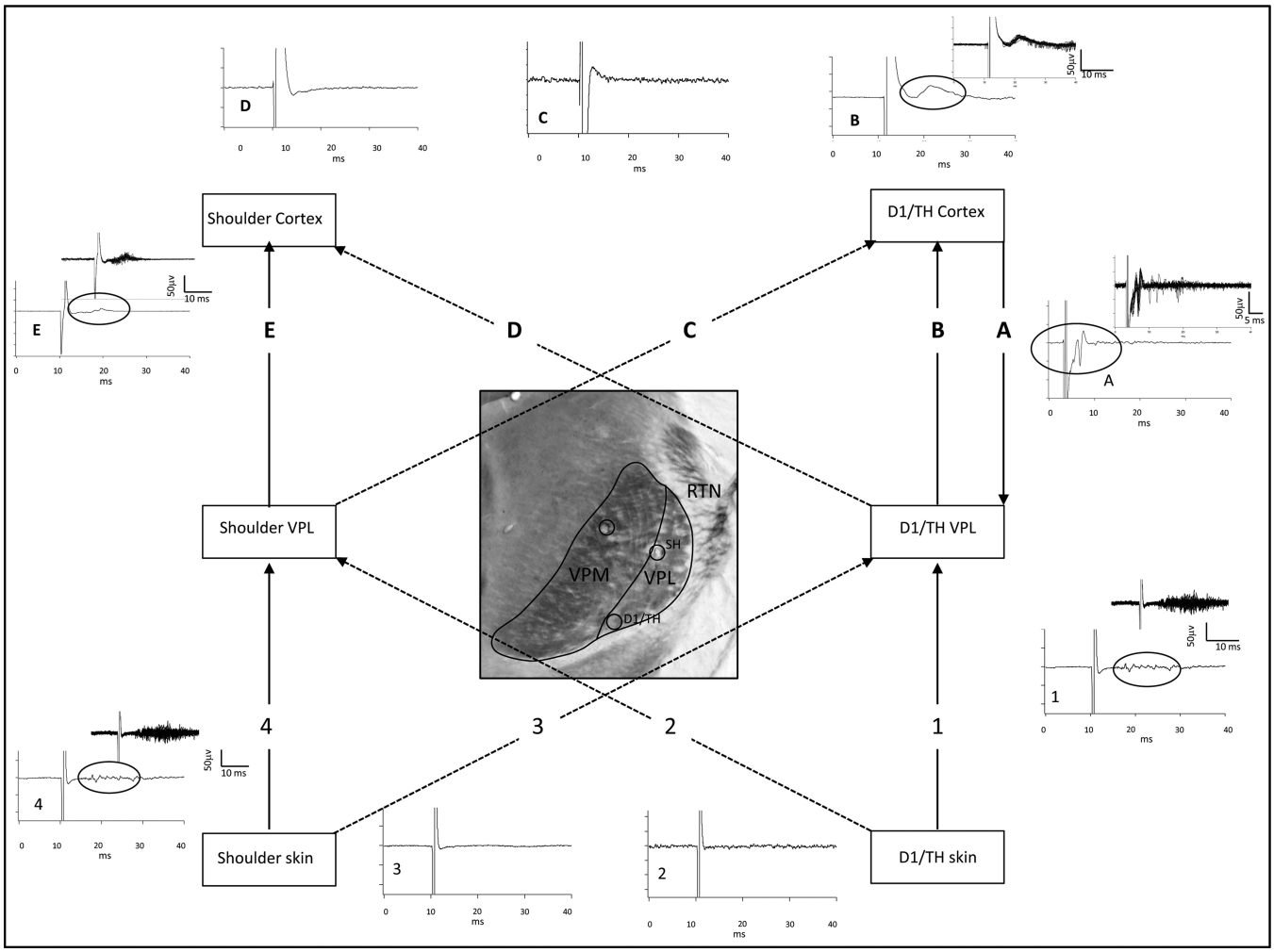

Fig. 3.

Pattern of projection from digit and shoulder periphery to VPL (nos. 1–4) and from VPL to SI cortex (letters “A”–“E”). Locations of D1/TH and shoulder representations in VPL are shown in the photomicrograph of CO-stained VPL that were identified by stimulating the digit and shoulder skin surface as described in Fig. 2. Stimulation of D1/TH evoked a response in D1/TH region in VPL (solid line labeled “1”) but did not evoke a response in shoulder sites (dashed line labeled “2”) in VPL. Similarly, stimulation of the shoulder skin evoked a response in a homotopic shoulder region in VPL (solid line labeled 4) but did not evoke a response in the digit region in VPL (dashed line labeled “3”). Averaged traces are shown for each of the stimulating and recording sites. Traces 1 and 4 show averaged evoked responses for 10 consecutive stimulations; circles in the trace indicate the evoked response part of the record. Insets show a response buffer for these traces. Locations of the D1/TH and shoulder representations were also identified in SI. The recording electrodes in VPL were then used to deliver single-pulse stimulation and responses were examined at digit and shoulder locations in SI (letters “A”–“E”). Stimulation at the digit location in VPL evoked a response in the homotopic digit location in SI (solid line labeled “B”) but not in shoulder location in SI (dashed line labeled “D”). Stimulation at a shoulder responsive site in VPL

evoked a response in the homotopic shoulder location in SI (solid line labeled “E”) but not in the D1/TH representation in SI (dashed line labeled “C”). Averaged traces are shown for each of these stimulation sites and buffers are displayed for those sites where evoked responses were recorded. The electrode in SI was then used for stimulation and the electrode in VPL was used for recording. An example of an antidromically-activated response is shown in trace “A”, but similar stimulation in shoulder SI failed to activate this digit site in VPL (data not shown).

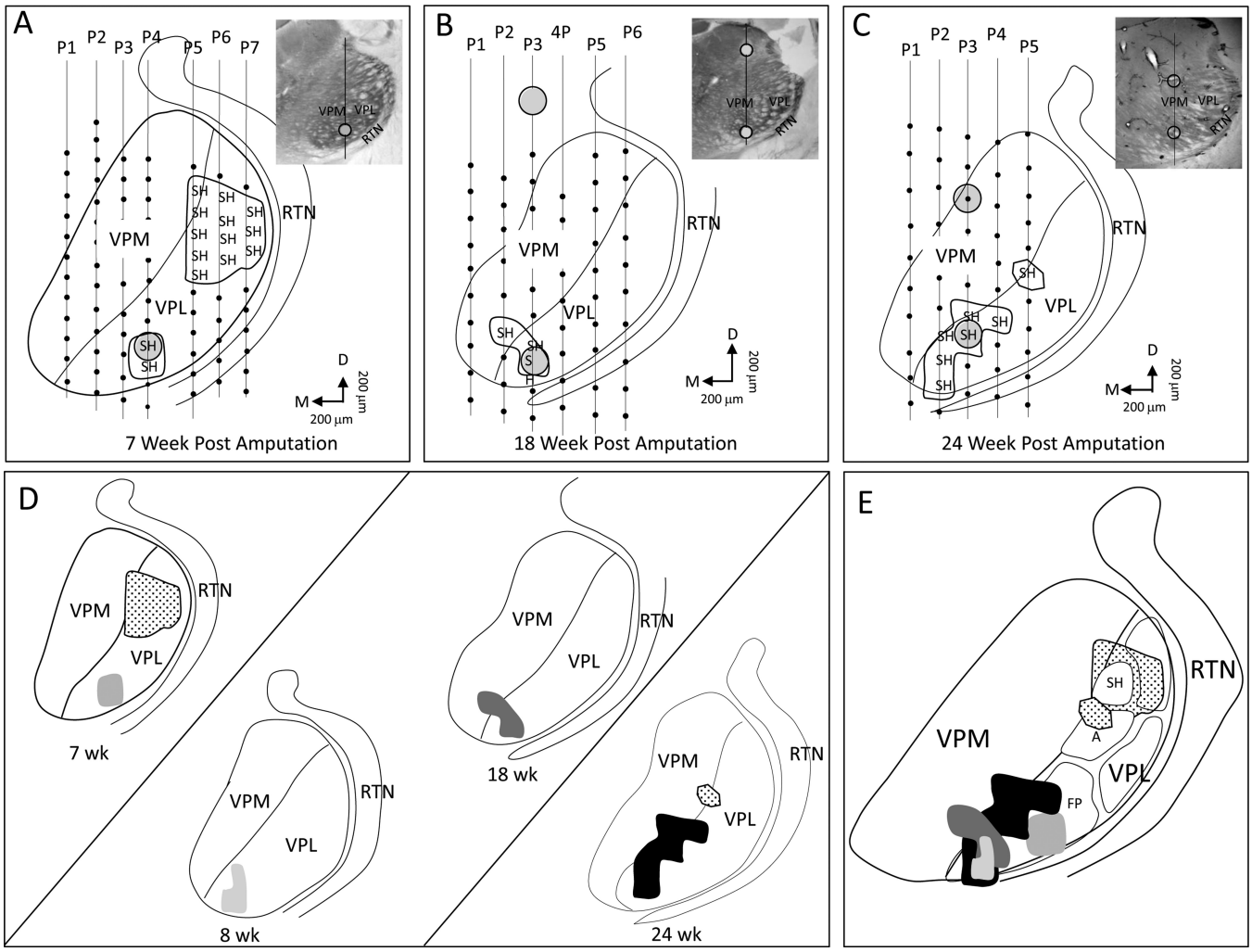

Fig. 4.

Photomicrographs, reconstructed line drawings, and interpretative summary of the reorganization in VPL at 7–24 weeks after forelimb amputation. **A:** Line drawing reconstruction showing a single row of 7 electrode penetrations that passed through VPM and/or VPL in an adult rat that was mapped 7 weeks post amputation. In penetration no. 4, the electrode recorded new shoulder input in the presumptive forepaw VPL. Penetration nos. P5–P7 recorded shoulder responses in the original shoulder representation. **B:** Example of a series of a single row of electrode penetrations in another rat that was mapped 18 weeks after amputation. New shoulder responses were recorded in the presumptive forepaw VPL. This row of electrode penetrations did not encounter receptive fields on the original shoulder representation but these were found in an adjacent row (data not shown). **C:** Another example of a single row of electrode penetrations from a rat mapped 24 weeks after amputation. In this rat, shoulder receptive fields were recorded in both the original shoulder representation (P5) and forepaw VPL (P2–P4). Insets show photomicrographs of CO-stained sections corresponding to the line drawings. Circles in both line drawings and photomicrographs designate lesions. **D:** Line drawing reconstructions from examples “A–C” and another rat mapped 8 weeks after amputation. **E:** Receptive fields for original and new

shoulder superimposed on the standard map of VPL (see Fig. 1). A = arm; FP = forepaw; SH = shoulder. Orientation arrows: M = medial; D = dorsal.

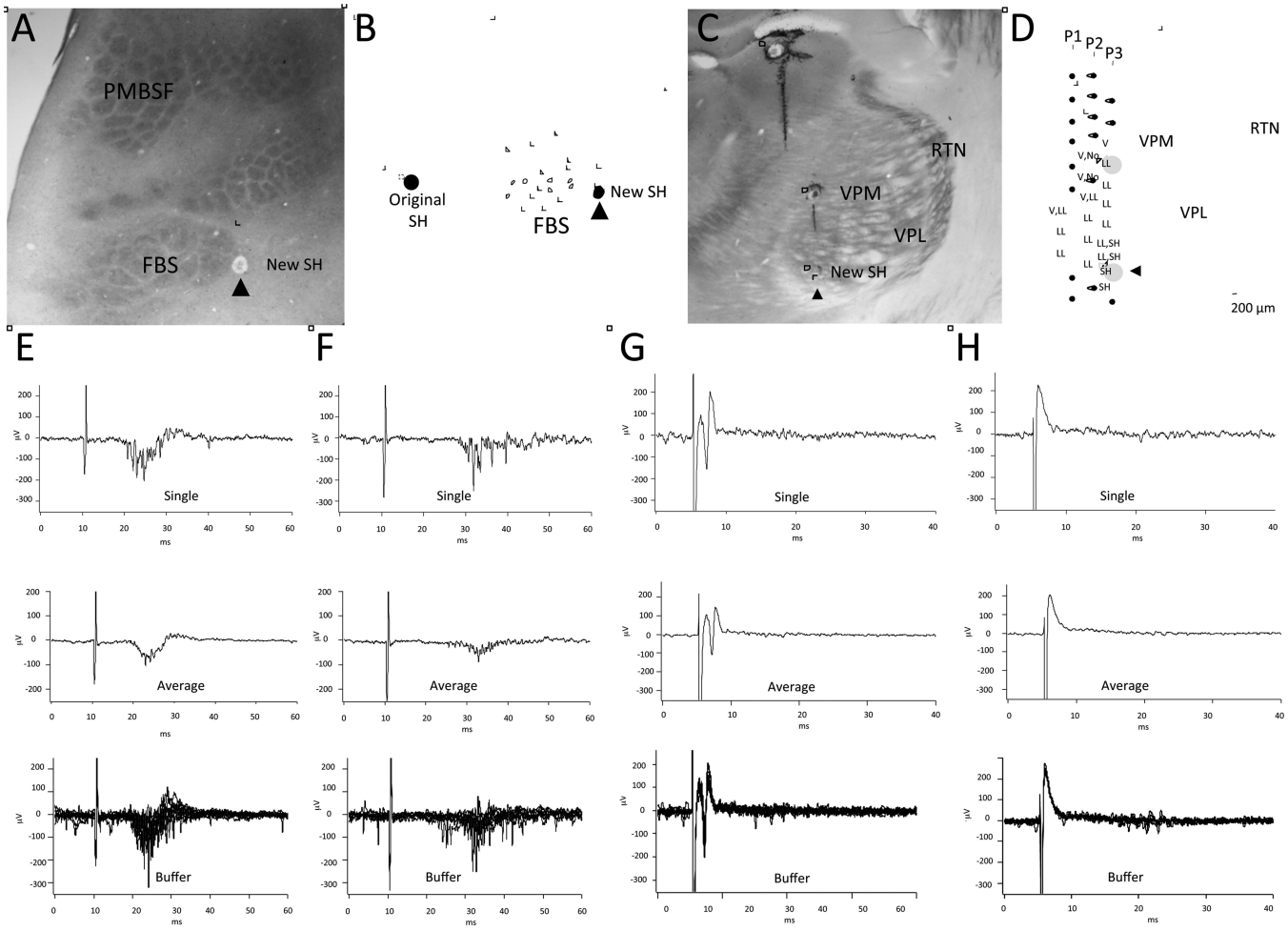

Fig. 5.

The former forepaw region in VPL provides a substrate for new shoulder input in deafferented FBS. **A:** CO-stained section showing the location (arrowhead) where a new shoulder response was recorded in deafferented FBS. This FBS site corresponds with the representation of D1 and TH pad. **B:** Line drawing of the barrel field showing the location where the new shoulder response was recorded in the FBS that was reconstructed in part from the CO-stained section in "A" where the lesion (black circle) was identified. The brain was blocked in this rat so both cortical and thalamic recording sites could be reconstructed. The dashed lines represent our estimation of the missing part of the barrel field. This part of the barrel field was drawn for placement of the location of the electrode track for the original shoulder representation that was obtained from the surface map of the brain in relationship to the position of the recording electrode in the FBS. **C:** Photomicrograph of a CO-stained section showing the recording site in VPL where a new shoulder response was recorded in the presumed former forepaw region in VPL that responded to new input from the shoulder. Open circles show locations where lesions were made along electrode penetrations. **D:** Line drawing showing electrode penetrations (P1–P3) in thalamus and recording sites in VPL where new shoulder responses were recorded in VPL. The ventral most lesion (open circle) in penetration no. 3 indicates the site selected for examination of the thalamocortical

projection to the FBS. **E:** Evoked responses recorded in the original shoulder representation in SI following electrical stimulation of the shoulder. Top record shows a single oscilloscope trace, middle record shows an average of 10 traces, and the lower record shows a buffer of 10 consecutive traces. **F:** Evoked responses recorded in the location of the new shoulder representation in the FBS following electrical stimulation of the shoulder. Note the longer latency for the initiation of the evoked response in the new shoulder representation as compared to the latency recorded in the original shoulder representation as previously described (Pearson et al., 1999). **G:** The electrode in the FBS was then used to deliver microstimulation and antidromically-activated responses were recorded from the electrode in VPL. The top trace shows a single oscilloscope trace, middle record shows an average of 10 traces, and lower record shows a buffer of 10 continuous stimulations. **H:** Stimulation from the original shoulder representation in SI did not elicit antidromically-activated responses in the recording site in VPL. Single, average, and buffer records are shown.

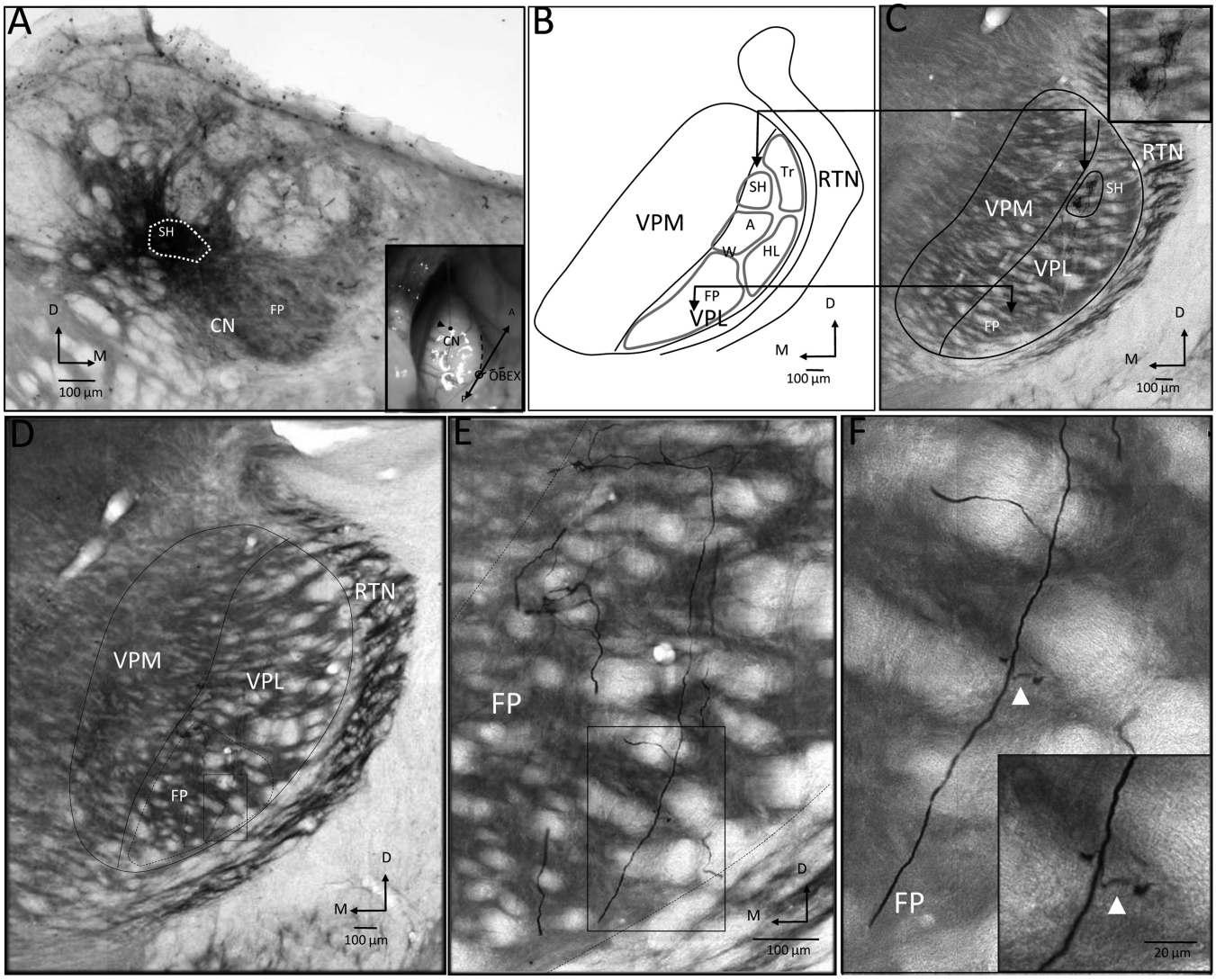

Fig. 6.

Projection pattern of BDA-labeled fibers following injection into the shoulder representation in CN in a forelimb intact rat. **A:** Photomicrograph of a coronal section through CN showing the location of the inner dense core of the injection site (dashed oval). Inset shows the surface location (arrowhead) where the recording electrode entered CN. **B:** Summary reconstruction showing the somatotopic organization of VPL from Fig. 1D. A = arm; FP = forepaw; HL = hindlimb; SH = shoulder; Tr = trunk; W = wrist. **C**: Photomicrograph showing labeling (enclosed oval) in the shoulder region in VPL. Inset shows terminal label in SH at higher magnification. **D**: Photomicrograph showing fibers branching in the vicinity of FP (dashed oval); the boxed region is expanded in **E** and **F**. Insets show magnified view of axon branches. Arrowheads in **F** show swellings likely associated with terminal labeling or axonal branching.

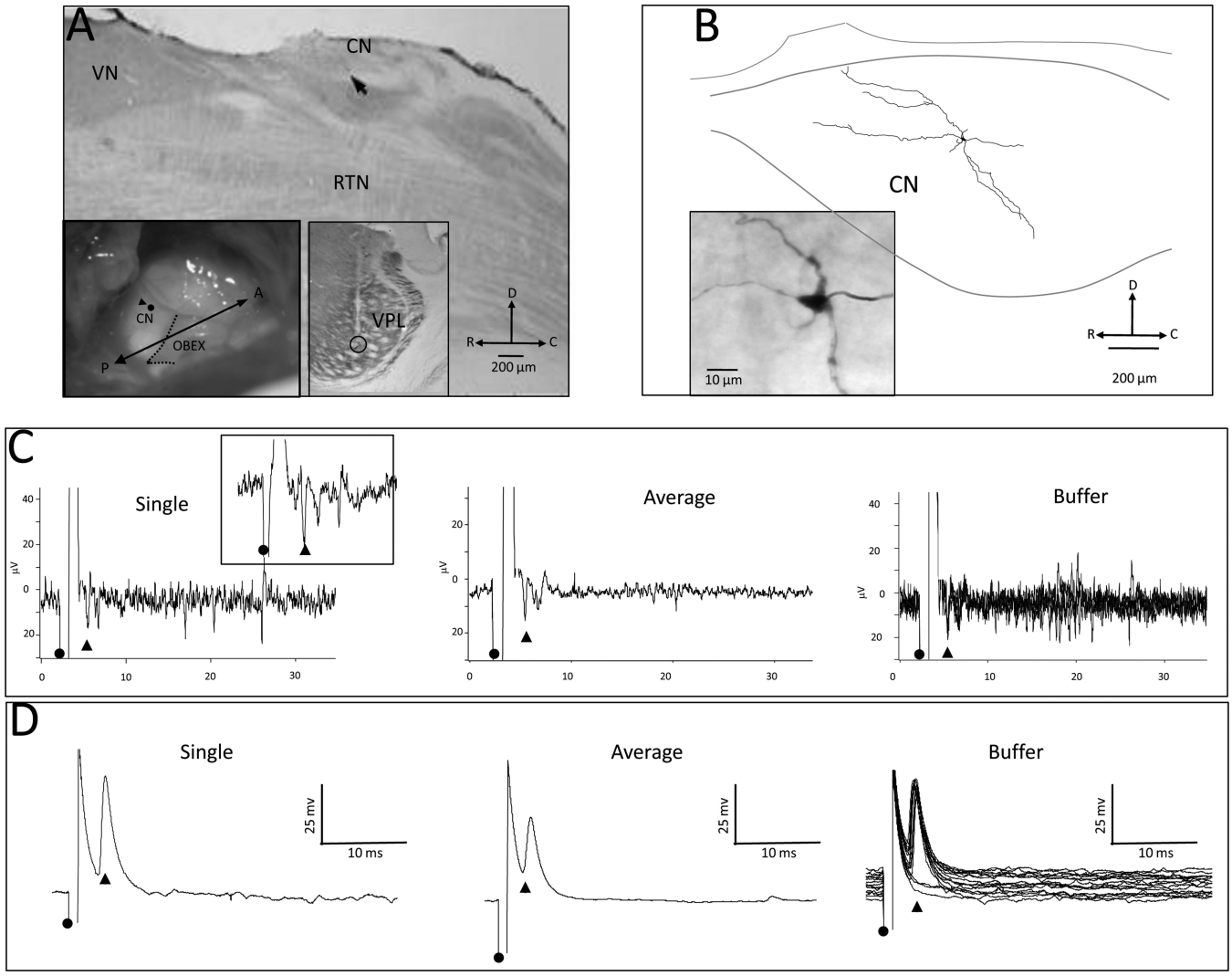

Fig. 7.

CN cells within the shoulder representation project predominately to the shoulder zone in VPL but also to forepaw and arm zones within VPL of forelimb intact rats. **A**: Photomicrograph of a sagittal section showing the surface location (arrowhead) where the recording electrode entered the brainstem and an antidromically-activated response was recorded in CN following stimulation in a physiologically identified site in the forepaw representation in VPL. Inset (left) shows a surface view of the brainstem and the surface point of entry (black circle) of the recording electrode into CN. Inset (right) shows the location of a lesion at the stimulating site in the VPL forepaw representation. RTN = reticular formation nucleus; VN = vestibular nucleus. **B**: Reconstruction of an antidromically-activated neuron in CN; photomicrograph in the inset shows the labeled cell. **C**: Extracellular traces showing an antidromically-activated cell (arrowhead); onset of stimulation is shown by the black circle. The left panel shows a single trace, the middle panel shows an average of 10 traces, and the right panel shows a buffer of 10 consecutive traces. The inset shows a single trace at a higher resolution. **D**: Intracellular traces recorded from a neuron at the approximate location of the extracellular traces in C. The left panel

shows a single trace, the center panel shows an average of 10 traces, and the right panel shows a buffer of 10 consecutive traces. This neuron had a spike height of 54 mV.

Table 1

Projection pattern from periphery to SI, VPL to SI, periphery to VPL, and SI to VPL

SI Cortex						
		Forepaw	***Wrist***	***Arm***	***Upperarm***	***SH***
Periphery to cortex	*Forepaw* *Wrist* *Arm* *Upperarm* *SH*	yes	NR	NR	NR	NR
		NR	yes	NR	NR	NR
		NR	NR	yes	NR	NR
		NR	NR	NR	yes	yes
		NR	NR	NR	yes	yes

SI Cortex						
		Forepaw	***Wrist***	***Arm***	***Upperarm***	***SH***
VPL to cortex	*Forepaw* *SH*	yes	NR	NR	NR	NR
		NR	NR	NR	yes	yes

VPL				VPL			
		Forepaw	***SH***			***Forepaw***	***SH***
Periphery to VPL	*Forepaw* *Wrist* *Arm* *Upperarm* *SH*	yes	NR	**Cortex to VPL**	*Forepaw* *Wrist* *Arm* *Upperarm* *SH*	yes	NR
		NR	NR			NR	NR
		NR	NR			NR	NR
		NR	NR			NR	NR
		NR	yes			NR	yes